DOE/MC/29106 -- 5262
(DE96011348)

Reprocessing Of Seismic Shear Wave And Tidem Data Collected At The A&M Areas Of the Savannah River Plant

Final Report
September 1992 - December 1995

March 1996

Work Performed Under Contract No.: DE-AC21-92MC29107

For

U.S. Department of Energy
Office of Environmental Management
Office of Technology Development
Washington, DC

U.S. Department of Energy
Office of Fossil Energy
Morgantown Energy Technology Center
Morgantown, West Virginia

By
Blackhawk Geosciences
301 Commercial Road, Suite B
Golden, Colorado 80401

Disclaimer

ABSTRACT

The upper aquifers in the A&M area of the Savannah River Site are known to be contaminated by chlorinated solvents. Remediation plans depend critically on continuity of a confining zone known as the Crouch Branch Confining Unit (CBCU), which occurs at depths between about 250 feet and 300 feet. Under DOE Contract No: DE-AC21-92MC29, administered by Morgantown Energy Technology Center (METC) surface and borehole geophysical methods were tested and further developed between 1993 and 1995 to map the lithology (clay content) and stratigraphy of the CBCU. It was found that time domain electromagnetics (TDEM) soundings were effective in mapping lithology and changes in lithology, and shear (S-) wave reflection surveys were effective in mapping stratigraphy. An integrated interpretation of the two methods yielded a rather complete image of lithology and stratigraphy of the CBCU.

At the completion of the 1993-1995 work, several issues needed to be further developed. Chief among those were:

- Seismic reflection prospecting with compressional (P-) waves dominates the seismic industry, and shear (S-) waves are far less used, except for such objectives as fracture mapping. As a result, little computer code is available for processing S-wave data. Moreover, the propagation characteristics of S-waves are less well understood. The unavailability of computer codes hindered effective processing of our shear wave seismic data.
- It was felt that more information could be derived from the TDEM data by constraining inversions with knowledge about the position of seismic horizons. In particular, obtaining values of resistivity for the CBCU with a low range of equivalence was an important objective.

Additional funding was obtained under Amendment No: 009 of the DOE contract to address some of the outstanding issues. This report contains the results of the additional work performed under Amendment No: 009. Extensive computer code was developed for more effective processing of multi-component S- wave high resolution reflection data. To test these algorithms and to better understand S-wave propagation in the near surface, multi-component check shot surveys were acquired in boreholes. The developed algorithms were mainly tested on the multi-component borehole data set.

The results of this analysis show clear evidence of seismic azimuthal anisotropy in the upper 300 feet of sediments of the A&M area. Evidence for anisotropy is seen in the splitting of horizontally polarized S-waves into fast and slow S-waves propagating with perpendicular particle motions. Furthermore, the azimuths of the fast and slow S-waves particle motions appear to correspond to the trends of major structural features in SRS. This suggests the near surface stress fields may be due to slumping of sediments into the Dunbarton Basin.

The development and application of the processing algorithms was more complicated than initially expected. For that reason, more effort was directed to code development and testing than to processing and interpretation. An important result is a rich library of software code to process S-wave data with the code integrated into existing processing packages. These packages have already been employed on other government and commercial contracts.

Also to derive additional information from TDEM data acquired, the data was reprocessed by constraining inversions by the position of seismic horizons derived from S-wave reflection surveys. The reprocessing resulted in more reliable values of the CBCU Resistivity values, in turn, can be correlated to clay content and vertical permeability. The inversions of the constrained data displayed considerably less equivalence than the unconstrained data, illustrating the advantages of employing more than one geophysical technique to accomplish certain objectives.

Finally, the value of the technical approaches developed under the DOE program is evidenced by the fact that presently routine surveys are being conducted by Blackhawk Geosciences in the A&M area for Westinghouse SRS funded under EM-40.

ACKNOWLEDGMENTS

We gratefully acknowledge the Department of Energy Morgantown Energy Technology Center for this project's major funding and in particular Vijay Kothari, DOE Project Manager. We are grateful to the Westinghouse Savannah River Company and in particular Carol Eddy-Dilek, Bob Van Pelt, and Brad Pemberton for their valuable help in coordinating field activities and providing us with existing information.

TABLE OF CONTENTS

LIST OF TABLES

FIGURE CAPTIONS

1. INTRODUCTION

Between 1993 and 1995, geophysical surveys were conducted over the A&M area of the Savannah River Site under DOE Contract: DE-AC21-92MC291076. The dominant objective of these surveys was to define the continuity and hydrogeologic characteristics of the Crouch Branch Confining Unit (CBCU). This confining unit occurs at a depth of about 300 feet below surface. Two geophysical data sets were acquired:

1. a time domain electromagnetic (TDEM) survey. In a TDEM survey, the geoelectric section of the subsurface is measured.
2. a high resolution shear wave reflection survey.

In comparing the interpretation of the geophysical surveys with geophysical, stratigraphic, and lithologic logs of wells, it was concluded that:

1. From the TDEM survey, the conductance (ratio of thickness and resistivity) of the CBCU could be derived which correlates to lithology.
2. From the high resolution shear wave reflection survey, the stratigraphy, i.e. the geometric relations between layers, beds and formations, was determined, such as abrupt variations (e.g. by erosion) and faulting was derived.

An integrated interpretation of both surveys, together with all data from available well logs, yielded the cross-section along line 1 shown in Figure 1-1. In this figure, the changes in lithology (soil types) are derived from the TDEM data, and the structure on the CBCU is obtained from the high resolution shear wave survey.

At the conclusion of the main body of work, several issues needed to be further resolved to refine the integrated interpretation of the CBCU in the A&M area, and to more effectively process multi-component seismic data. Some of the required work was performed under Modification A009 of the above referenced contract and this report deals with the work performed under that Modification. The results of the work under the main contract was previously reported on.

Important objectives of the extension of the contract work were:

1. To refine the classification of lithology of the CBCU shown on Figure 1-1. In particular to make an attempt to correlate resistivity to clay content and hydraulic parameters, such as vertical permeability. The principle procedure for accomplishing that was to constrain TDEM inversions by the high resolution seismic reflection data to derive independently thickness and resistivity of the CBCU, and to in turn correlate resistivity to clay content.
2. To more effectively process 4-component surface shear wave reflection data, to observe any birefringence in the data, and to correlate birefringence to geotechnical properties of the CBCU. To better resolve the principals of shear wave components and to determine the existence of shear wave anisotropy, multi-component check shot surveys were run in five boreholes, and new algorithms for processing were developed for these tasks.

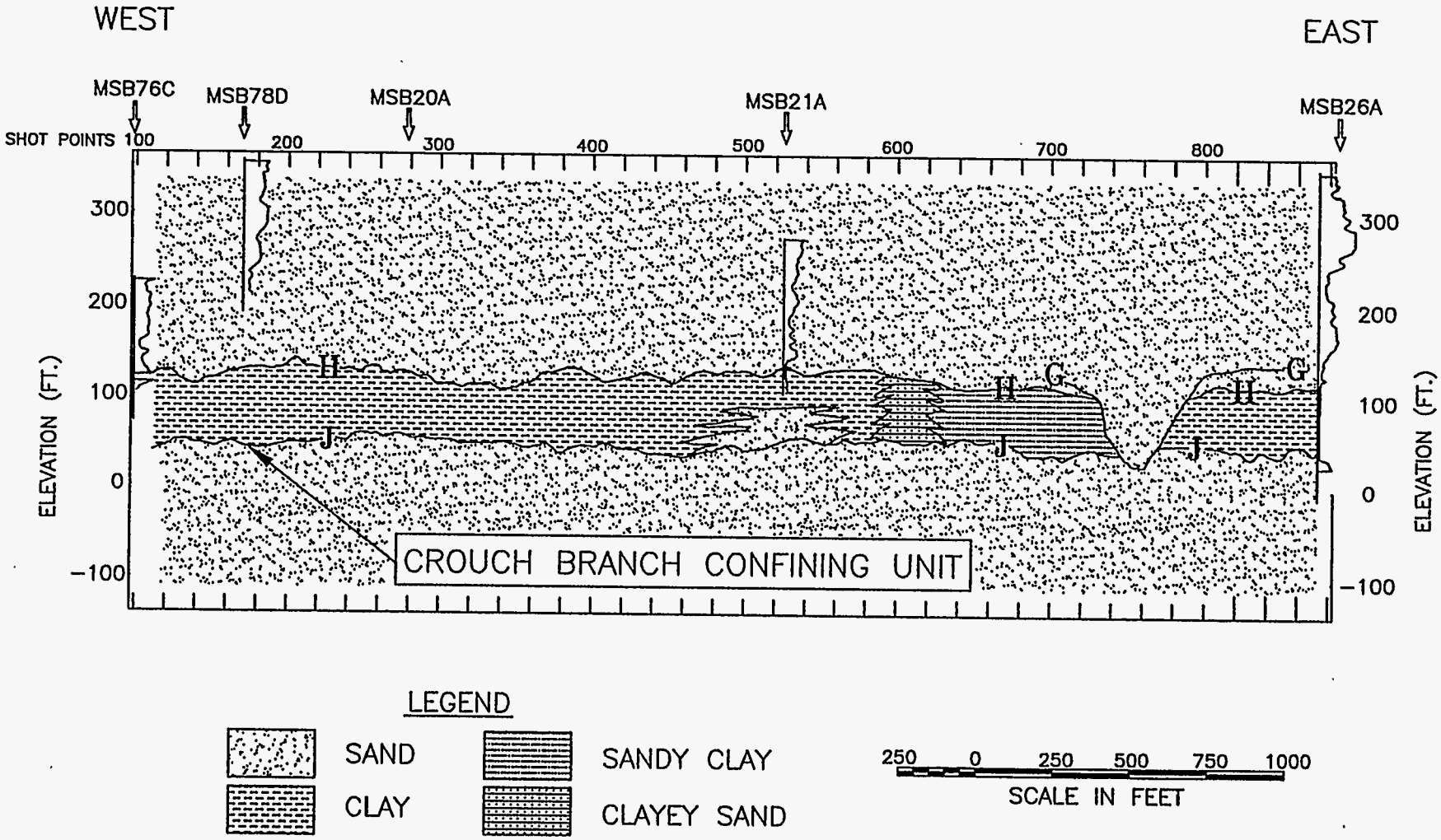

Figure 1-1. Line 1: Geologic section derived from integrated interpretation of TDEM geoelectric sections, seismic sections, core, and geophysical logs. The CBCU occurs between reflectors H and J and is continuous along the line except where cut by a channel between Points 720 and 800. Note the facies change between Points 580 and 720.

In Section 2, the reprocessing of the TDEM data and the correlation of resistivity to clay content are discussed. In Section 3, the acquisition of multi-component borehole checkshot surveys is described, the development of algorithms for processing multi-component data sets are detailed, and the results obtained from applying these algorithms to shear wave downhole survey data acquired under this contract are given.

In Section 4, we review the commercial opportunities for the technologies developed. Some of the commercialization potential has already resulted in additional commercial contracts.

2. TDEM REPROCESSING

2.1. Geoelectric Section of the A&M Area

In TDEM the geoelectric section of the subsurface is measured. Characteristics of the geoelectric section typical of the A&M area can be understood from the resistivity logs run in wells (Figure 2-1) . The two-well logs illustrate that the CBCU has distinctly different electrical resistivities from the rest of the section, and that the electrical resistivity varies considerably across the CBCU. The CBCU represents a thin layer of low resistivity (caused by clays) in a resistive section (dominantly sands).

Figure 2-2 can be used to explain the rationale for further processing of the TDEM data. On the left side of Figure 2-2 the geoelectric section derived from 1-D inversion of a sounding near borehole MSB26A is superimposed on the resistivity log run in that hole. On the right side of the figure the cumulative conductance's derived from the resistivity log and the TDEM soundings are shown. The observations from this comparison can be summarized as follows:

- There is good agreement in the behavior of the cumulative conductance curves derived from the TDEM sounding and the borehole resistivity log. In both data sets the dominant contribution to the cumulative conductance in the upper 130 m (400 feet) of the section is from the CBCU clay unit.
- The TDEM geoelectric section derived from the unconstrained 1-D inversion indicates the top of the CBCU clay unit at the correct depth, but is not accurate in predicting the thickness of the clay. The resistivity value of the clay is 10 Ω-m derived from the TDEM, compared with an average of 135 Ω-m for the well log. The thickness of the clay is 50 feet compared with 85 feet for the well log.

2.2. Constrained Inversions

The objective of constraining the inversion process by stratigraphic information from seismic surveys is to separately resolve resistivity and thickness of the CBCU. In turn absolute values of resistivity can be correlated to clay content and clay content perhaps to vertical permeability.

To derive more accurate estimates of the CBCU resistivity from the TDEM data, and to attempt to correlate TDEM resistivity to clay content, the following processing procedure was followed:

- The elevations of the top and bottom of the CBCU (taken from the seismic data) were used to constrain the elevation of the CBCU in the TDEM inversions.
- Grain size data (supplied by WSRC) was compared to constrained TDEM resistivity and borehole resistivities over the CBCU interval.
- The TDEM data taken along Lines 1 and 2 (reference Figure 1-1) were reprocessed with constrained 1-D inversions. Over the west portion of Line 2 where seismic data was not available, the elevation of the top and bottom of the CBCU was estimated using data from Boreholes MSB43 and MSB29.

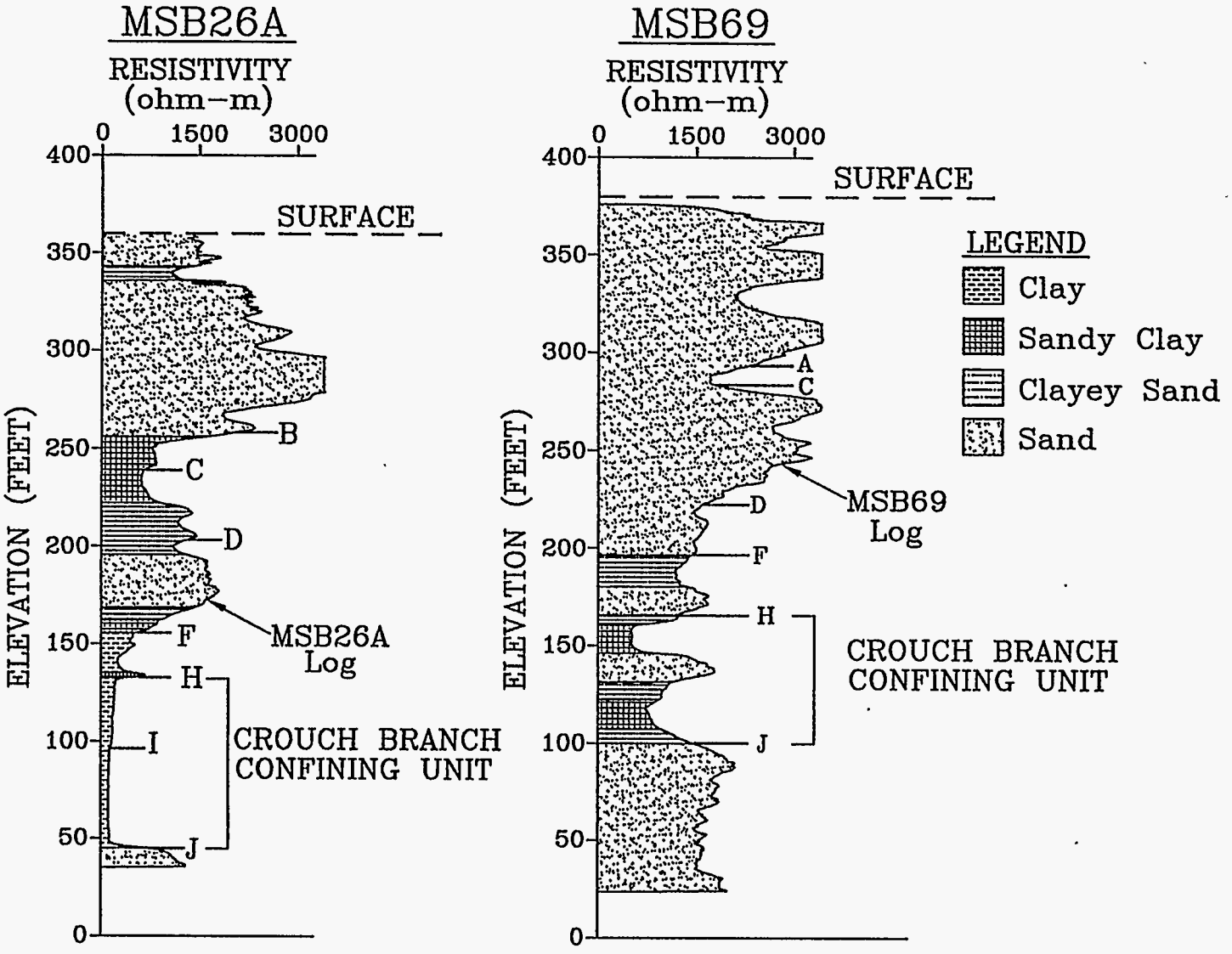

Figure 2-1. Two typical borehole resistivity logs, soil types from core descriptions, location of the Crouch Branch Confining Unit. Note difference in depth thickness and electrical resistivity of the CBCU between the two wells which are 9,000 feet apart.

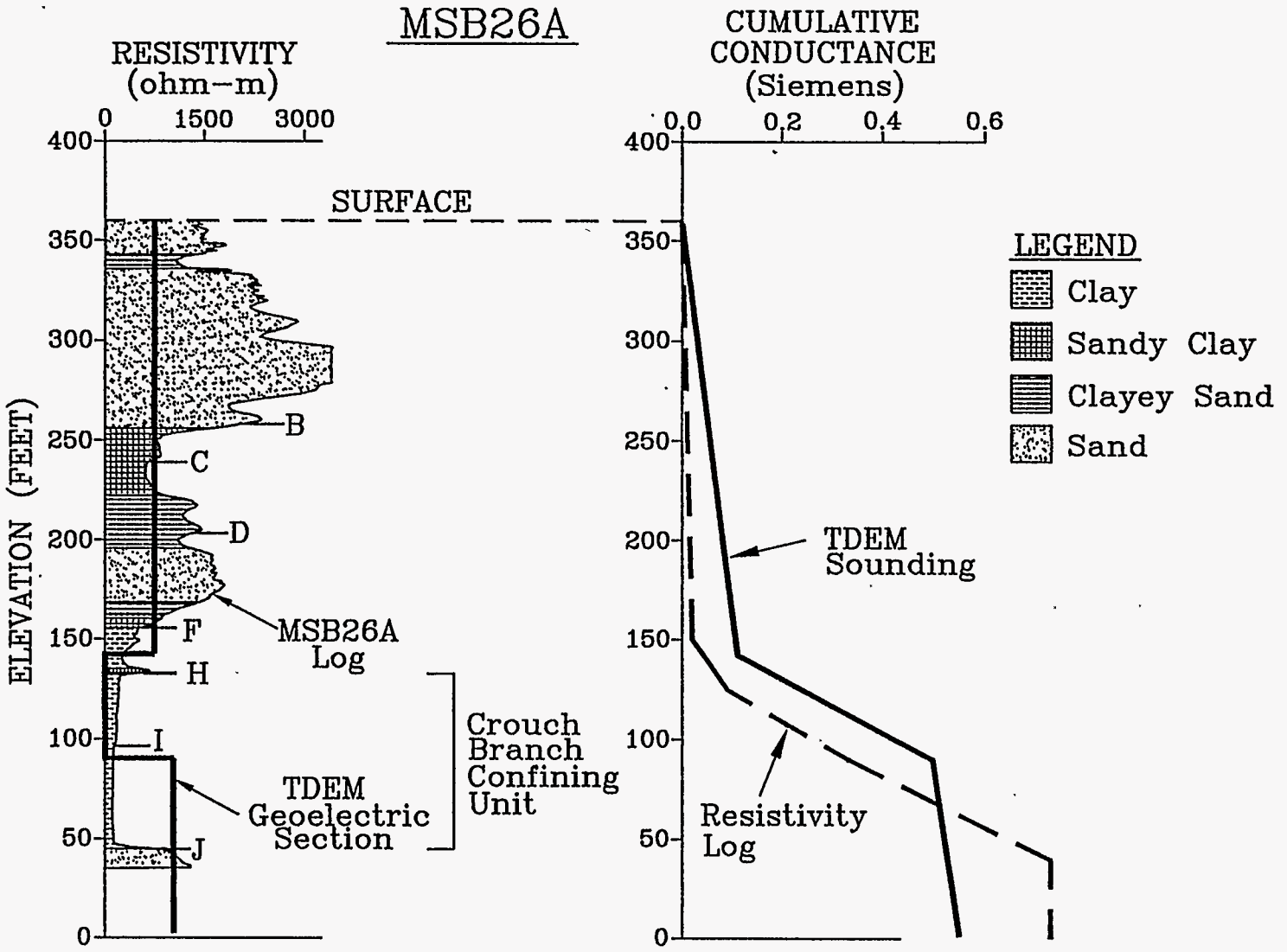

Figure 2-2. Comparison of geoelectric parameters derived from borehole resistivity log, and 1-D inversion of TDEM sounding. Left: vertical geoelectric profile from the TDEM sounding superimposed on the resistivity log; Right: cumulative conductance calculated from the TDEM sounding and the resistivity log.

Figure 2-3 compares the 1-D inversion results for a typical TDEM Sounding (7284Z, Line 1) using an unconstrained inversion (Figure 2-3a), and the constrained inversions (Figure 2-3b). In both the constrained and unconstrained inversions, the percent error between the best fit forward model and data (left side of figure) is less than 5%, indicating that the solutions (geoelectric sections) derived from both inversion types fit the data equally well.

For both constrained and unconstrained inversions, an equivalence analysis was performed. In an equivalence analysis all solutions that match the observed data within a specified RMS error are computed. The RMS error used in the analysis is 5 %. The critical parameter of interest is the resistivity of the CBCU. As shown in figure 2-3, the equivalence in the resistivity of the CBCU is greatly reduced by constraining the inversion by knowledge from the seismic survey and borehole data. The results of constraining the inversions along lines 1 and 2 are shown in Figures 2-4 and 2-5. In these figures the absolute value of resistivity of the CBCU is shown by a shaded gray scale grid.

2.3. Correlating the Resistivity to Clay Content

The constrained inversion yields resistivity values for the CBCU within narrow error bounds. For hydrogeologic investigations resistivity values in turn must be correlated to clay content. There are several relationships between clay content and resistivity published, but these relationships depend on clay mineralogy and are regional specific. To establish a relationship specific to the A & M area the grain size distribution in two wells was correlated to resistivity logs run in wells. Borehole resistivity logs were not corrected for borehole diameter or variations in porewater conductivity. The grain size data for two wells in the A&M area was provided by WSRS. For deriving clay content the percentage mud (size fraction less than 0.0625mm) was used, and this size fraction was equated with clay content. Figure 2-6 shows the relationship between borehole resistivity and per cent mud. The borehole resistivity logs were not of the best quality. There are questions about calibration of the tool and missing sections. Figure 2-6, however, shows that within a particular hole, there is a consistent correlation between resistivity and percent mud. The behavior of the relation is similar between the two holes, but the absolute values deviate. We expect the main cause of this to be due to variation in tool calibration, however variations in clay mineralogy could also contribute.

2.4. Conclusions on Reprocessing of TDEM Data

Constraining inversions of TDEM data by stratigraphy derived from seismic data results in resistivity values for the CBCU with a small range of equivalence. Correlating borehole resistivity values to clay (mud) content in two boreholes resulted in relationships that clearly shows the dependence of resistivity of the CBCU on mud content, but the absolute values of resistivity differ between the two holes. The deviation is expected to be due to differences in tool calibration, missing sections, or mineralogical change.

We believe that reliable borehole logs and hydraulic tests can result in establishing relationships between resistivity (as measured by TDEM) and clay content. Clay content in turn can be correlated with vertical hydraulic conductivity.

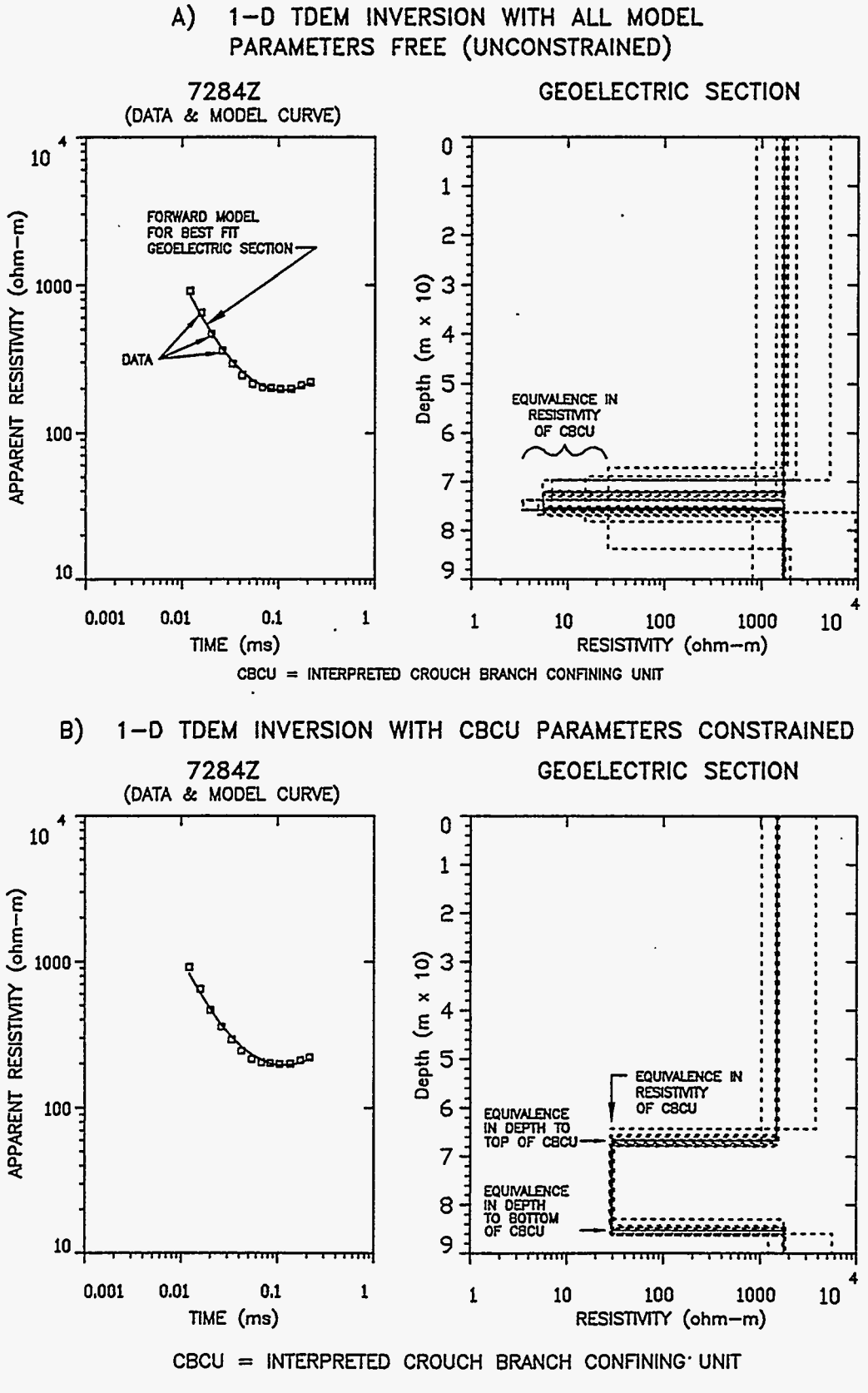

Figure 2-3: Comparison of Unconstrained and constrained TDEM 1-D Inversions. A&M Area, Savannah River Site.

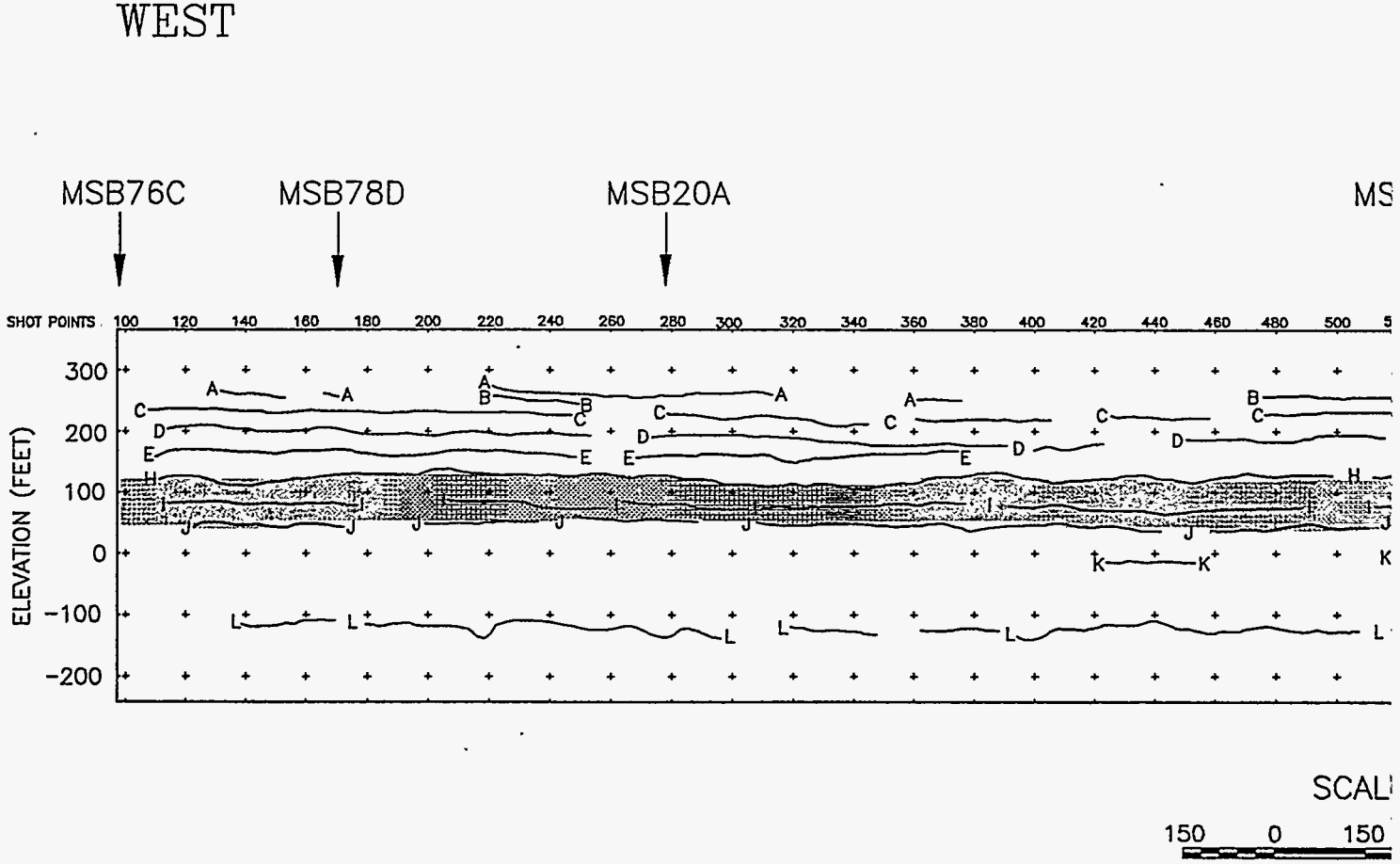

Figure 2-4. Results of constrained inv
was to better resolve the absolute val
Confining Unit, and the resistivity valu

LN1RES.GRD
\PROJECTS\SAVAN5\LINE1\BASEFNL.PLT

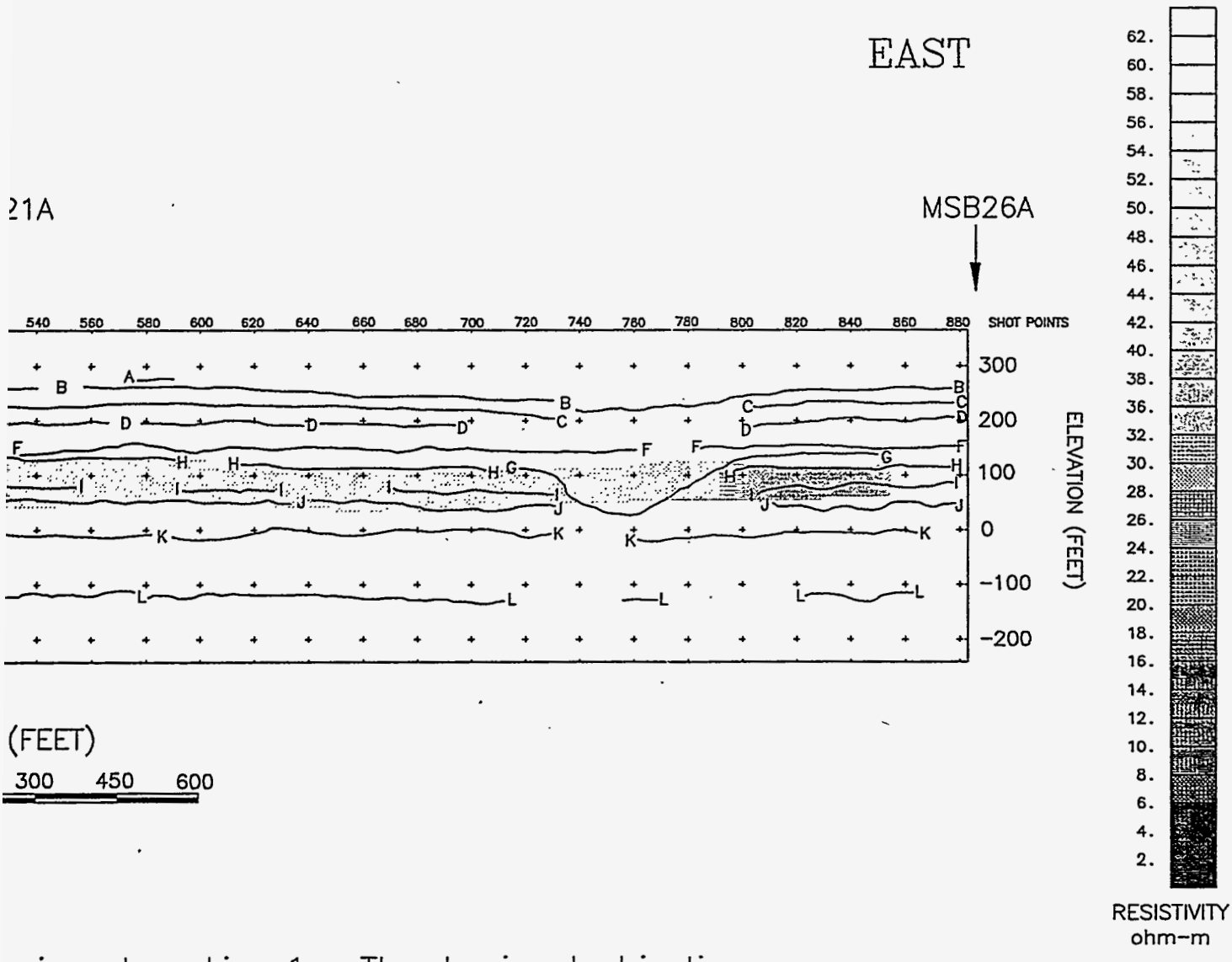

ersion along Line 1. The dominant objective
e of resistivity of the Crouch Branch
es are displayed by a grey scale shading.

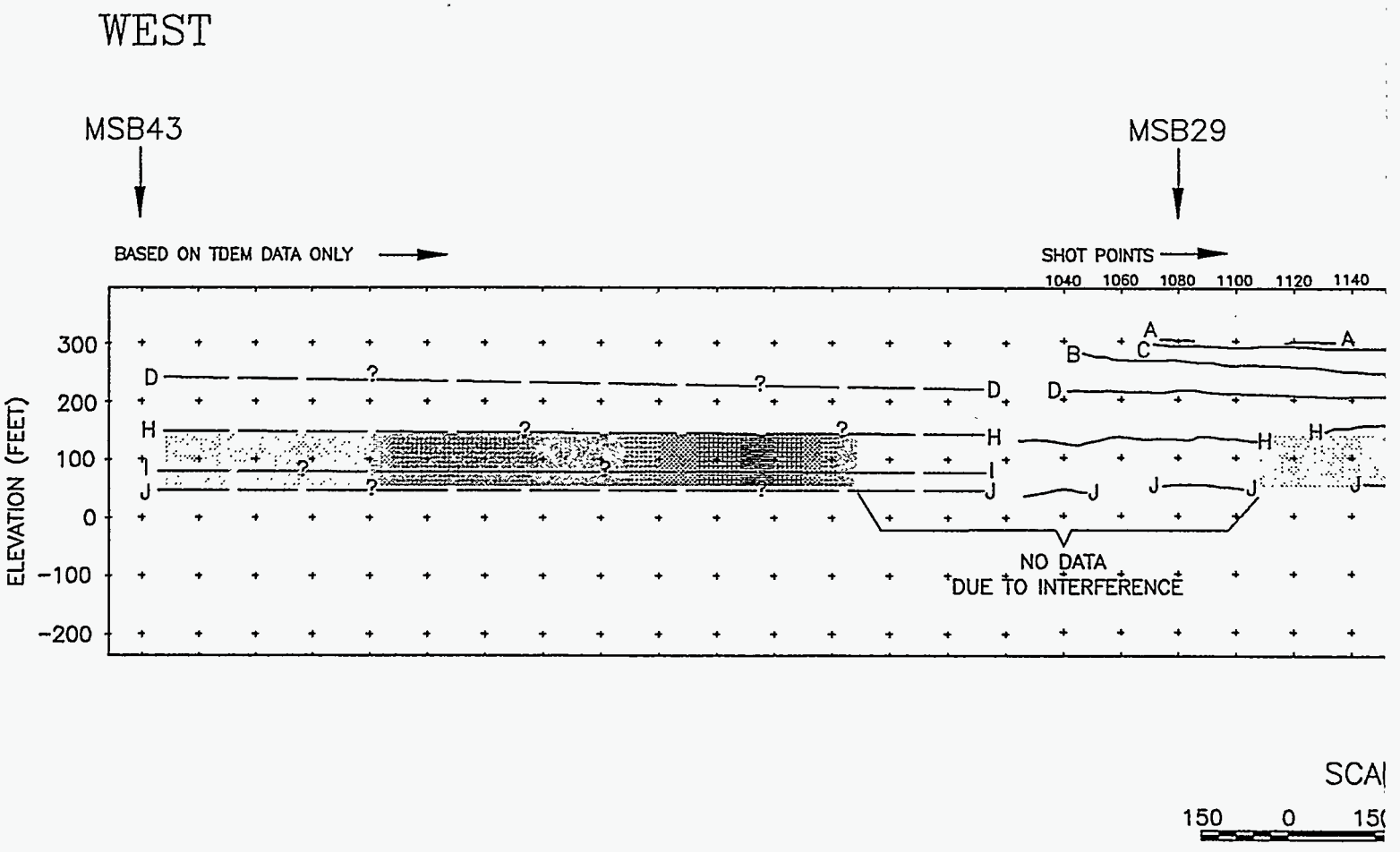

Figure 2-5. Results of constrained inver
was to better resolve the absolute value
Confining Unit, and the resistivity values

RESGREY.GRD
\PROJECTS\SAVAN5\LINE2\BASEFNL.PLT

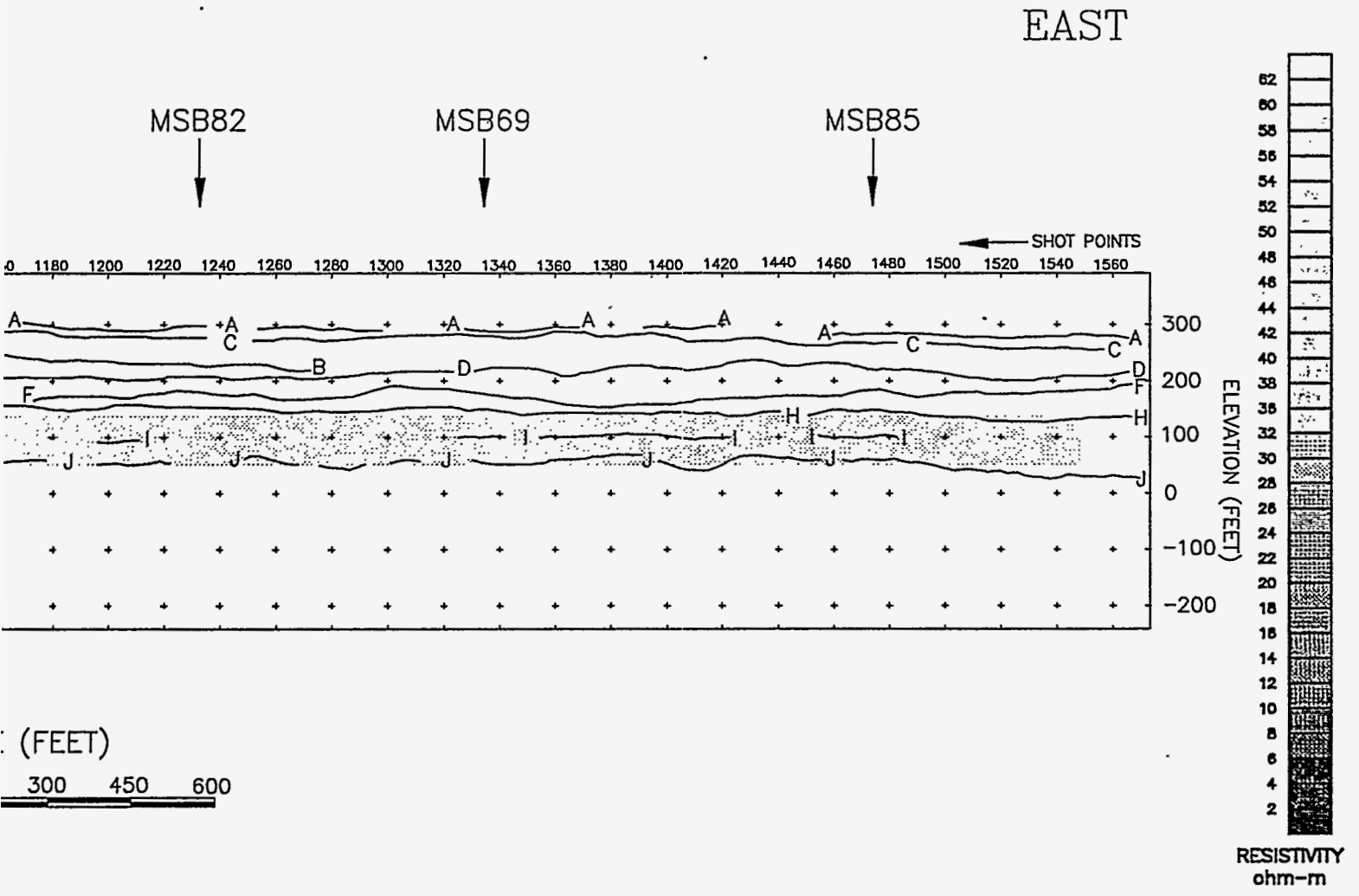

on along Line 2. The dominant objective
of resistivity of the Crouch Branch
are displayed by a grey scale shading.

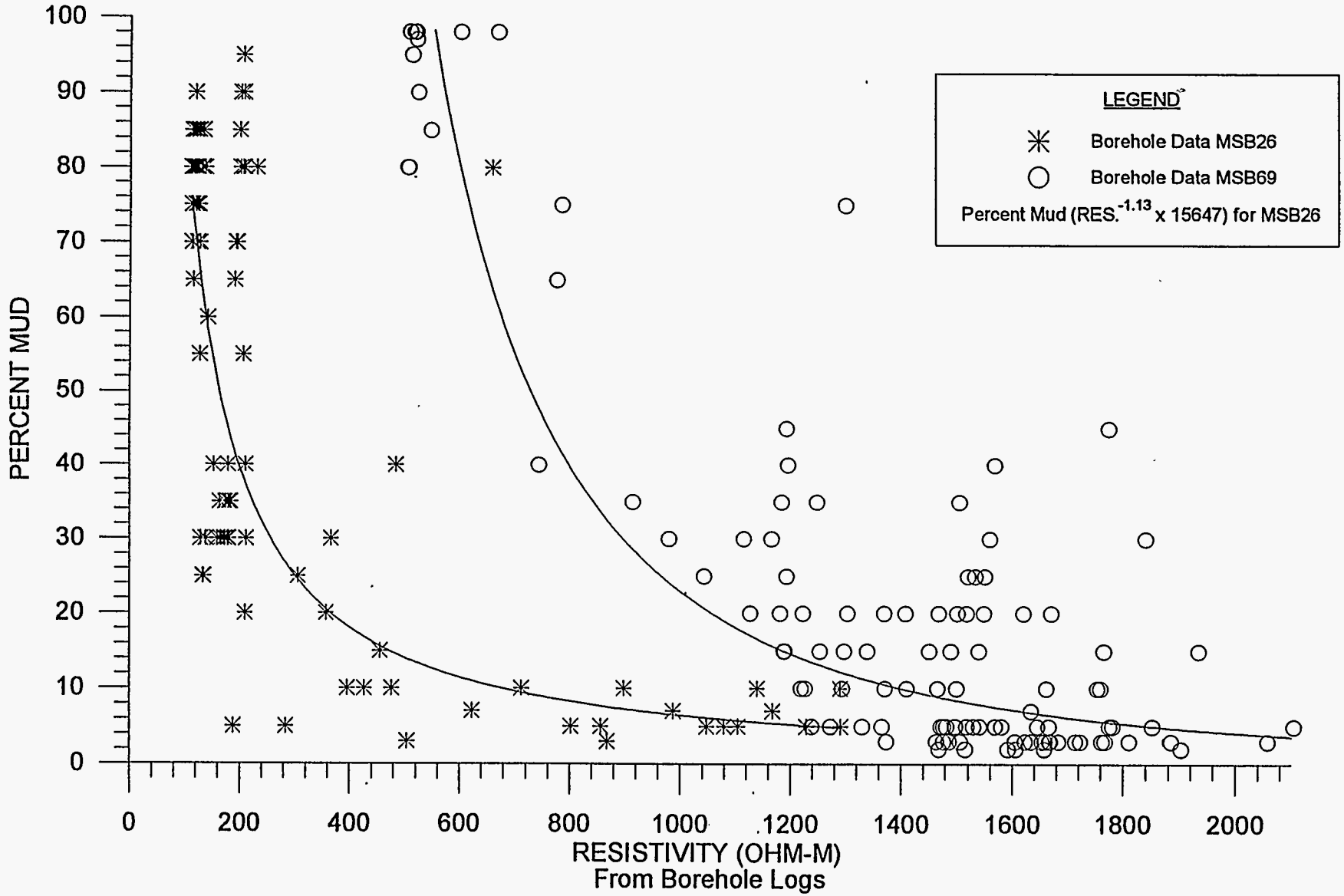

Figure 2-6: Borehole resistivity versus percent mud for boreholes MSB26 and MSB69. A&M Area, Savannah River Site.

3. SEISMIC SHEAR WAVE DATA ACQUISITION AND PROCESSING

The major goal of this study has been to discover evidence of seismic anisotropy at the Savannah River Test Site, and to characterize the most important properties of the anisotropy including magnitude and orientation. Determining the presence of seismic anisotropy and its characteristics could result in several benefits including:

- Improved processing of multi-component surface shear wave reflection data.
- Constraining the geometry and possible location of near surface faulting.
- Inferring information of lithologic parameters(clay content) from anisotropy parameters.

Downhole data were recorded on three-component geophones using S-wave and P-wave sources at five different well locations. The S-waves are diagnostic of anisotropy and were used for this purpose. The P-waves were used to orient the geophones.

There are a number of methodologies that have been developed to analyze shear wave birefringence. Each of these methodologies depend on certain simplifying assumptions, and each methodology displays differing sensitivity to noise. Several of the techniques that are commonly used in the oil and gas exploration industry for detection of fractures are a principal cause of anisotropy and were coded and applied to the downhole data at SRS. To gain an appreciation of the limitations of these methods, we also applied each method to a synthetic data set, and also to synthetic data sets that were purposely corrupted. Such exercises provide insight into interpretational errors which can occur due to breakdown of assumptions.

The downhole data was collected in five different wells at numerous depths. Altogether, four-component recordings were obtained for 183 distinct source-receiver combinations. The synthetic VSP data set (Model 1) was provided by the Edinburgh Anisotropy Project. We consider the asynchronous rotation method of Igel and Crampin (1990), and the standard Alford rotation method (Thomsen, 1988). The comparisons obtained from these methods are useful since each method yields the same result for the synthetic data but yields somewhat different results for the real data.

In this section, we will discuss the data acquisition of the borehole data, the development and testing of the algorithms used to process multi-component data and the results from our analysis of the borehole data. Estimates of the fast shear wave direction and the magnitude of anisotropy were made for all the borehole surveys. Geologic information which may be obtainable from these measurements is also discussed.

3.1. Data Acquisition of Borehole Checkshot Survey

A downhole geophysical survey was performed at the SRS by Blackhawk Geosciences from 11/29/95 to 12/2/95. The objective of the survey was to measure the shear wave velocity field in the subsurface, as well as determine the direction of the fast and slow S-waves, and the degree of anisotropy.

The boreholes selected for the downhole velocity surveys are located along two shear wave seismic lines surveyed by Blackhawk in 1995. The locations of the shear wave lines and the boreholes are shown in Figure 3-1. Boreholes MSB-21TA and MSB-26TA were located along seismic line 1. Boreholes MSB-69TA, MSB-29TA, and MSB-43TA were located along line 2. Table 3-1 shows when each hole was surveyed and the total depth surveyed.

Table 3-1

Downhole Seismic Shear Wave Surveys

Borehole	Total Depth Surveyed	Date
MSB-21TA	306 ft	11/29/95
MSB-26TA	186 ft	11/30/95
MSB-69TA	300 ft	11/30/95
MSB-29TA	246 ft *	12/1/96
MSB-43TA	306 ft	12/2/95

* 60 Hz noise was encountered at a depth of 120 feet in this well, and the signal/noise ratio decreased rapidly with depth below 120 feet. All attempts to mitigate this noise were unsuccessful, and the data quality below 140 feet is poor.

Downhole Survey Acquisition Parameters

The following procedures were followed for the shear wave velocity surveys in each well. A far offset compressional wave (P-wave) source location was chosen to be used for orientation of the horizontal elements in the downhole geophone. Offsets for the P-wave sources were typically 100 to 200 feet away from the borehole.

Three shear wave (S-wave) source positions were chosen. These source positions were all located 10 feet from the borehole at 60 degree increments. The shear wave source positions with respect to the borehole are given in Figure 3-2.

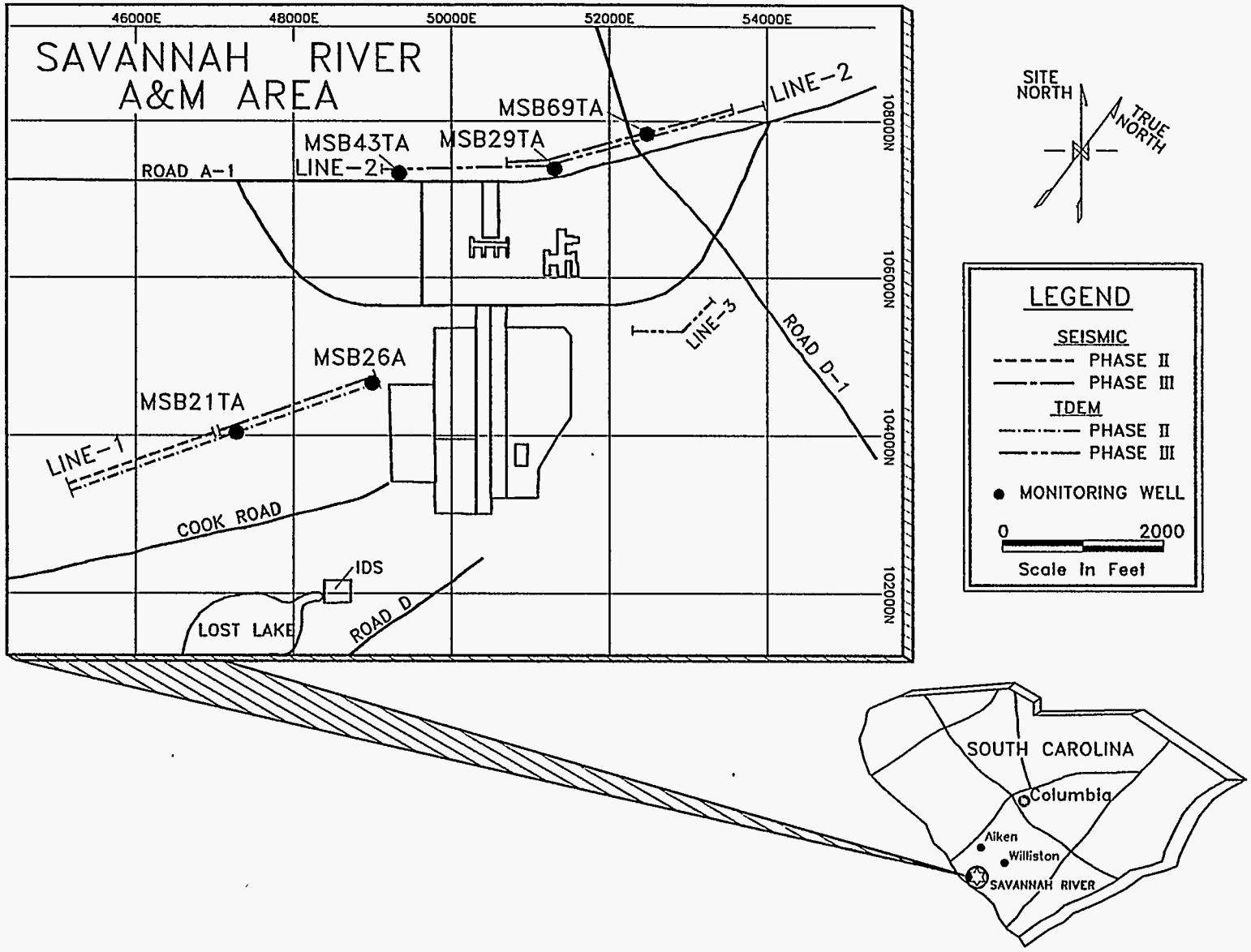

Figure 3-1. Location of downhole shear wave surveys.

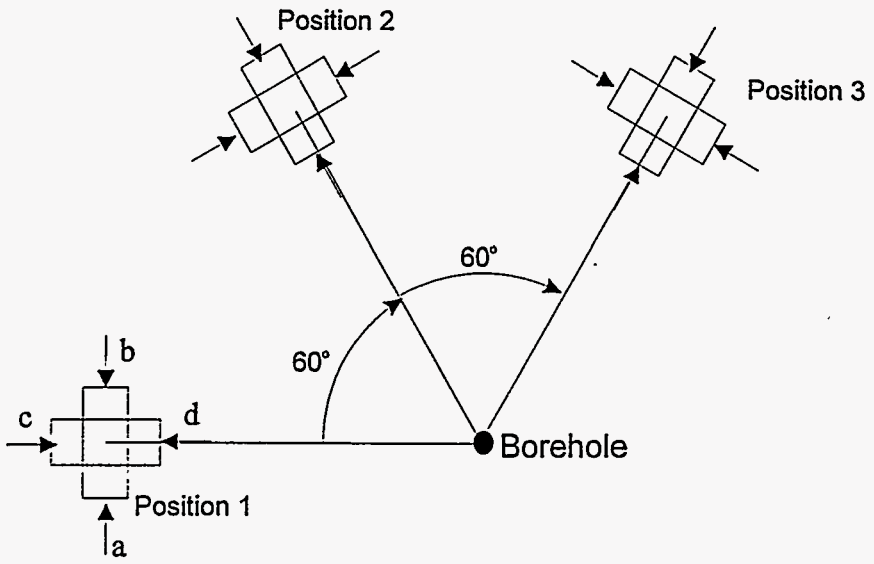

Shear Wave Source Positions **Figure 3-2**

After selection of source points, the OYO Borehole Shuttle was assembled and deployed in the borehole. The seismic data recording at each depth level proceeded from Step 1 through Step 6 as follows:

1. The three-component geophone is lowered to the desired depth and secured to the borehole walls via mechanical locking arms.
2. The P-wave source was impacted with a sledgehammer until clear breaks could be identified on the horizontal geophones. This seismic record was then written to the hard disk on the OYO DAS-1 seismograph and all geometry information recorded in the log book.
3. Shear wave position 1 was occupied. The shear source was impacted with a sledgehammer in a clockwise motion (shown as **a** on Figure 2-1) until a sufficient signal to noise ratio was achieved. This file was then written to the hard disk, and all shot and receiver location information were recorded in the log book. Shear components **b, c,** and **d** were then recorded in the same manner as described for **a.**
4. Shear wave position 2 was then occupied, and recordings **a, b, c,** and **d** were repeated.
5. Shear wave position 3 was then occupied, and recordings **a, b, c,** and **d** were repeated.
6. The geophone was unclamped and moved to the next recording level.

Recording proceeded in this manner until data had been recorded every 20 feet to the bottom of the borehole.

3.2. Shear Wave Processing Algorithms

To measure anisotropic parameters from shear waves in a downhole experiment (such as a VSP) or in seismic reflection survey, it is necessary to record at least two components of motion for a given shear-wave source. With two-component recordings, it is possible to recover the two most important characteristics of an azimuthally anisotropic medium, namely the fast direction of propagation and the magnitude of anisotropy. However, this approach tends to be less robust than four-component recordings in which orthogonal horizontal components are recorded for shear sources that are inline and crossline (i.e. the shear source is aligned along the line connecting source and receiver, and orthogonal to it). This is because two-component techniques will be more sensitive to noise (there is less redundancy in the data) and the analysis techniques that can be applied are more restrictive. It may be possible to use P-wave sources and interpret the converted shear arrivals, which reduces acquisition costs but can increase processing and interpretation costs, if the signal to noise ratio is poor.

To perform different types of seismic analysis (including the Alford rotation), it is necessary to define an inline-crossline recording geometry. In a four-component shear-wave acquisition geometry, the four trace recordings are defined as follows:

s_{11} = (inline-receiver component due to inline source)

s_{12} = (crossline-receiver component due to inline source)

s_{21} = (inline-receiver component due to crossline source)

s_{22} = (crossline-receiver component due to crossline source)

The recording geometry is shown in Figure 3-3.

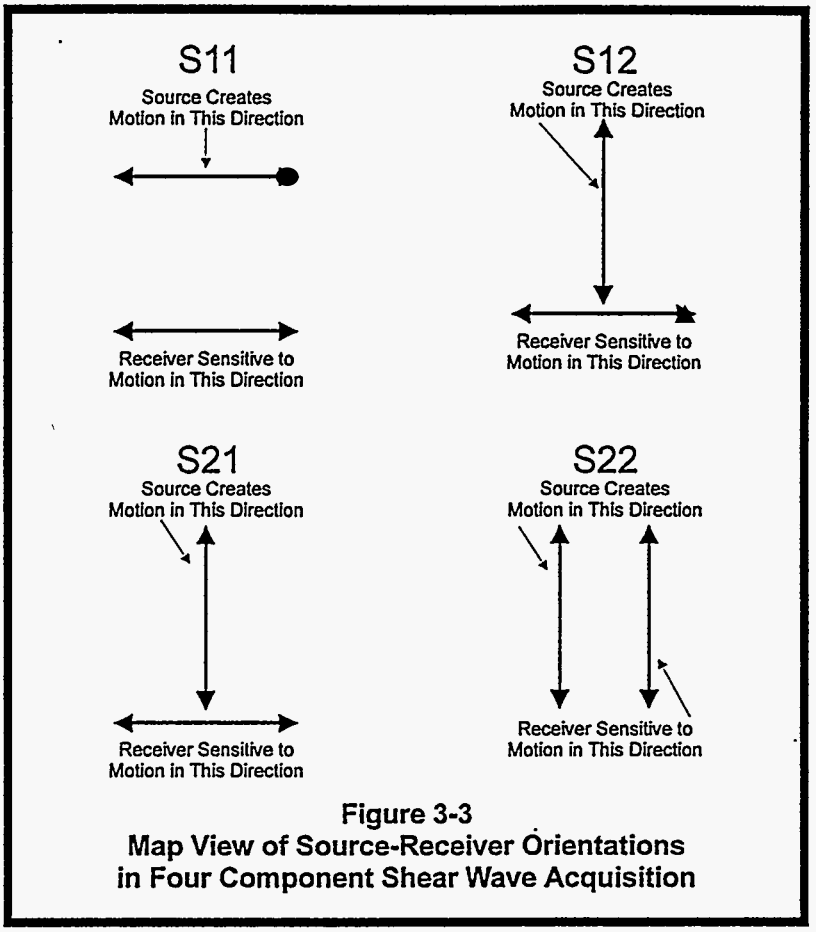

Figure 3-3
Map View of Source-Receiver Orientations in Four Component Shear Wave Acquisition

After analysis and rotation of the data into the natural coordinate system of azimuthal anisotropy, two principal time series are analyzed. The are defined as follows:

qs1 = principal time series along "fast" axis

qs2 = principal time series along "slow" axis

In this section we describe the data processing tools that were developed to analyze the downhole data. The programs were developed on a Silicon Graphics Indigo and Linux workstations, and data interaction and display was facilitated through use of SU (Seismic UNIX), developed at the Colorado School of Mines. In sections 3.2.1 through 3.2.6, we describe each of the processing sequences in detail; but in the following, we summarize the most salient elements:

- A low-pass **Butterworth filter** was applied to all traces to reduce high frequency noise. Roll-off began at 200 Hz.

- The far-offset P data were used to perform a geophone orientation or **toolspin correction**. This is necessary because the orientation of the geophone in the borehole is not known during data acquisition. The toolspin process computes the orientation of the geophones in the borehole. The three-component traces for each geophone were used to determine the appropriate P-wave window for this analysis. Four different methods were applied but all amounted to rotating the horizontal components until energy is minimized in the crossline direction (or maximized in the inline direction). The different estimates agreed to within a few degrees, when the plus or minus 180 degree ambiguity is accounted for. We resolved the ambiguity by requiring P-wave first breaks with positive polarity.
- The horizontal components of recordings from the **S sources were mathematically rotated to the inline-crossline geometry** using knowledge of the source azimuths and geophone orientation obtained from the toolspin correction.
- **First break shear wave windows** were determined for use in the Alford rotation analysis. Identification of these events was facilitated by plotting traces side by side for a given component generated by sources with opposite polarity. Arrivals with transverse motion will display opposite polarities when generated by such sources. This approach helps distinguish contribution from P-wave motion.
- An **Alford rotation analysis was performed** using as input the shear wave window of the first break, and a set of four traces for each geophone given by the crossline source and crossline receiver component (s_{11}), crossline source and inline receiver component (s_{12}), inline source and inline receiver component (s_{22}), and inline source and crossline receiver component (s_{21}). The angle that minimized energy on the mismatched traces was determined over the specified shear wave window. Using the angle obtained from this subwindow, the principal time series *qs1* and *qs2* for the entire input trace length were computed. In addition, for purposes of comparison, the original input data was synthetically modeled using *qs1*, *qs2*, and the fast direction. Thus, for each geophone six traces were output: the four synthetically modeled traces and the two principal time series. The rotation analysis is dependent on certain assumptions including that the input mismatched traces (*i.e.* s_{12} and s_{21}) are identical. Therefore, as a quality control check the correlation coefficient of the mismatched traces and their RMS energies in the shear wave window were computed.
- An alternate method of analyzing multiple component data using the **Asynchronous Rotation Method of Igel and Crampin** to determine the presence of azimuthal anisotropy and the azimuths of the *qs1* and *qs2* directions. This method is more general than the Alford rotation in that the source and receivers can be rotated independently; and therefore, the *qs1* and *qs2* directions can be different at the source and receiver locations. The method creates an energy spectrum which is a function of the source polarization and the horizontal direction. A histogram is then generated by summing over all the source orientations for many horizontal directions. These histograms will then display maximums in the *qs1* and *qs2* directions.

- **Cross-correllogram between the *qs1* and *qs2* principal time series** were computed. The *qs1* and *qs2* waveforms are expected to be similar but *qs2* should be time-lagged relative to *qs1*. The location of the positive peak on the cross-correllograms subtracted from the midpoint of cross-correlogram trace yields the time-differential between *qs1* and *qs2*. Depending on the nature of the recordings, either the *qs1* and *qs2* should be cross-correlated in their entirety, or the subwindow containing the first break on the *qs1* trace should be excised and cross-correlated with the entirety of *qs2*. The cross-correlogram is a useful quality control measure and aids to indicate the success of the Alford rotation. In general, the cross-correlogram should be symmetric about the positive peak, decay rapidly from this peak with increasing time lag. Otherwise, the waveforms are not likely to match well, or there may be considerable noise present.

3.2.1. Low Pass Filtering

A spectral analysis revealed that most of the energy in the P and S recordings was below 100 Hz; yet, in many cases there was clear evidence of high frequency noise. The appearance of the seismograms was considerably improved by applying a low-pass filter to all of the traces in the data set. For this purpose, we used a Butterworth filter with a cutoff frequency of 200 Hz. As discussed later, in some of the traces there was clear evidence of 60 Hz noise, undoubtedly from powerlines. We attempted to remove this component of the signal with a notch filter, but ultimately were unable to do so since much of the seismic signal is also near this frequency.

3.2.2. Geophone Orientation

The data were recorded with three-component geophones (horizontal-x, horizontal-y, and vertical-z). The downhole shuttle in which the geophones are mounted do not include measures for determining relative or absolute orientation of the horizontal axes. The shuttle twists and randomly orients the horizontal components from depth to depth. This random orientation must be removed by orienting the data to a fixed reference frame. This can be done by mathematically transforming the x and y components of the recorded data. As can be seen from Figure 3-4, the result of the transform is two new orthogonal traces are now be aligned to a specified reference frame.

We applied four different analysis methods to recover the true orientation of the geophone, and these are described in detail in the following section. The first method rotates the horizontal components of the recordings until the energy of the first break is maximized on one of the components. The second method is an analytical implementation of this condition. The third method is a histogram technique, and the fourth uses singular value decomposition to compute the principal polarization direction in the *x-y* plane from which the angle of propagation can be derived.

All of the methods rely on the particle motion of the P-waves remaining confined to the path defined by the source-receiver. Any out-of-plane motion due to heterogeneities will limit the accuracy of the toolspin correction. For some geophone depth levels, P-wave data were recorded using both 100 and 200 feet offset P sources. For these data the estimated toolspin corrections agreed to better than five degrees. Furthermore, each of the four methods described below yielded corrections angles that agreed to better than two degrees in all cases. Therefore, we believe that for the well sites considered, the ray-bending effects were minimal, and that five degrees represents an upper bound on the error for computing the orientation of the down hole tool.

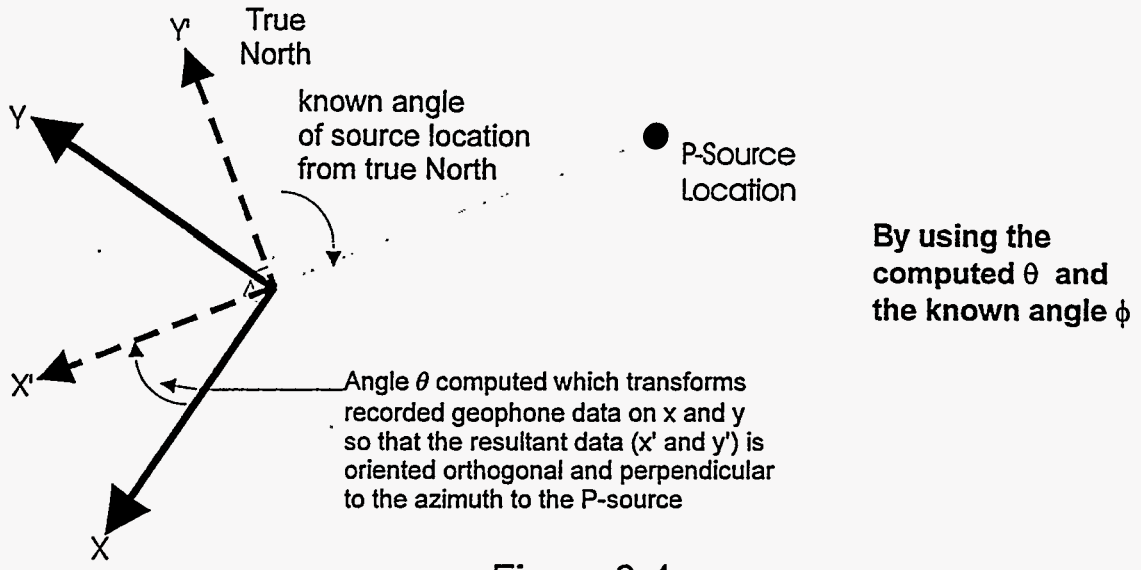

Figure 3-4
Geometry of Toolspin Orientation Computation

To establish an absolute coordinate system, we use information from far-offset P-wave sources. P-waves are produced by compressional sources, and the direction of the particle motion of these waves is collinear with the direction of propagation (the line connecting the source and receiver). The horizontal projection of the direct-arrival particle velocity is the same direction as the ray's surface projection from the wellhead towards the source. Defining the axes (x,y) to be original unknown axes for the geophone, (x',y') to be the axes in which x' is aligned with the line connecting source to receiver, and q to be the angle between x and x', then the coordinate transformation that rotates the (x,y) axes into the (x',y') axes is given by

$$x' = x\cos(\theta) + y\sin(\theta)$$

$$y' = -x\sin(\theta) + y\cos(\theta)$$

The effectiveness of the toolspin algorithm can be tested by mathematically rotating the two traces so that the geophones are oriented to the x' and y' axes. In this orientation, all energy from a far offset P-wave source should arrive on the x' axes and very little should be seen on the y' axes. This effect can be seen on the example shown in Figure 3-5, where the unoriented data has P-wave energy arriving on both traces, whereas the oriented traces only have energy on the trace oriented in-line with the azimuth to the P-wave source.

The four methods which we used to compute the angle q are discussed in the following sections.

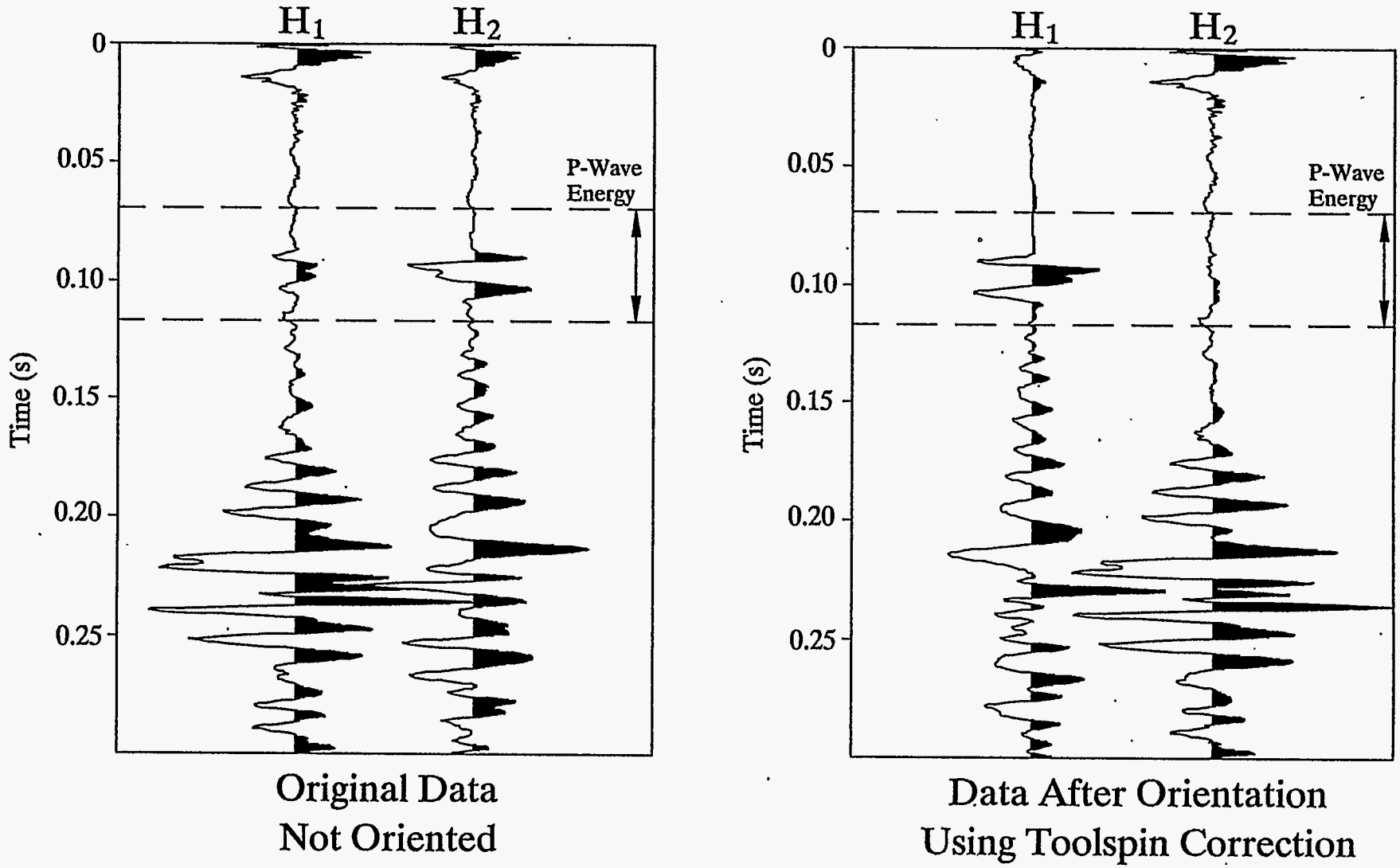

Figure 3-5. Comparison of traces before and after toolspin correction.

3.2.2.1. Energy Method

One of the techniques we applied to determine the appropriate angle q was to maximize the energy on a particular axis (the x' axis). For each trace, we chose a particular time window containing the first P arrival and computed the energy on the x' axis for a suite of rotation angles. The energy for angle q is given by

$$E(\theta) = \Sigma(x(t)\cos(\theta) + y(t)\sin(\theta))^2$$

where the sum is taken over all time points in the window. The energy function varies smoothly with q and the value that yields the greatest energy value is the appropriate angle.

3.2.2.2. Analytical Energy Minimization

The desired angle can also be found by estimating the angle in which the differential of the energy with respect to q is minimized. Define

$$X = \Sigma\, x(t)$$

$$Y = \Sigma\, y(t)$$

where the sum is taken over all time points in the window. Taking the derivative of $E(q)$ with respect to q, setting the result to zero, and solve for q, we obtain

$$\tan(2\theta) = 2XY / (XX\text{-}YY)$$

which analytically defines the angle that yields the minimum energy value.

3.2.2.3. Singular Value Decomposition

Another method which we used is by performing a polarization analysis of the P-wave recording. In this method, the two time series from the horizontal component over the first break are written to an $Nx2$ matrix, where N is the length of the time series A singular value decomposition (SVD) of the matrix was performed. The v eigenvector corresponding to the largest singular value also yields the dominant direction of motion. The appropriate angle θ was obtained by computing the arc tangent of the components of the vector *i.e.*,

$$\theta = atan\,(v_y/v_x).$$

3.2.2.4. Histogram Method

Finally, a histogram method was used in which the angle θ for each point in the time series was computed using the formula

$$\theta\,(t) = atan(y(t)/x(t))$$

where *atan* is the arc tangent function. A small binning interval for q was chosen, and a histogram was computed to obtain the distribution of q. The final value was chosen by obtaining the peak of the histogram distribution.

3.2.3. Polarity Correction

Each of the methods for toolspin correction described above align one of the horizontal axes of the geophones with the inline direction, but do not distinguish polarities, i.e. the methods yield results that are ambiguous by plus or minus 180 degrees. To resolve this ambiguity we require the first breaks of the P-wave arrivals on the inline component to have either a positive or a negative polarity. An algorithm was implemented to yield the desired polarity, but on average, yielded the correct polarity for about 90% of the traces. It was necessary to visually inspect the rotated P-wave recordings and make manual corrections to ensure complete consistency.

3.2.4. *Rotation to inline-crossline geometry*

In order to perform the standard Alford rotation analysis, it is necessary to work in a geometry in which the receiver elements are aligned (inline) and orthogonal (crossline) to the shear wave sources, which are also aligned (inline) and orthogonal (crossline) to the line connecting source and receiver. In the downhole study; shear sources were placed at three distinct azimuths about the well, each with ten feet offset.

However, for each geophone in each well only one P source was used to obtain the toolspin correction. To rotate the system to the desired coordinate system, it is necessary to associate the appropriate toolspin correction for each geophone depth and well. Then it is necessary to compute the difference in azimuths for the given P and S sources pairs. The appropriate rotation angle for geophone k in well j and shear source azimuth with index m is given by

$$\phi_{kjm} = \theta_{kj} + S_{kjm} - P_{kj}$$

where ϕ_{kjm} is the desired rotation angle, θ_{kj} is the toolspin correction for the unique P source, S_{kjm} is the azimuth of the S source for geophone k, well j, and source azimuth with index m, and P_{kj} is the azimuth of the P source for geophone k and well j. The first angle in the above formula rotates the coordinate system to an absolute reference defined by the azimuth of the P source, and the last two terms account for the difference in the S source azimuth relative to the P source azimuth. The relationship between these angles is diagrammed in Figure 3-6.

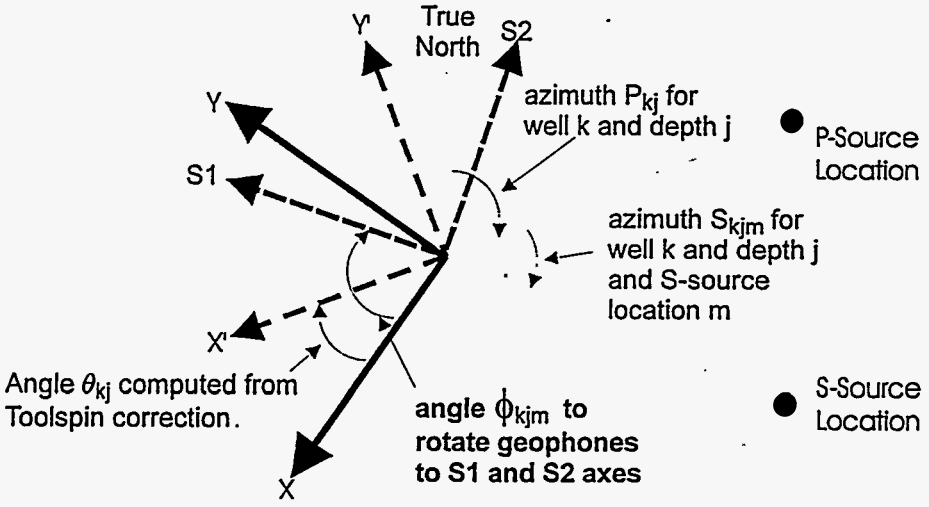

Rotation of Geophone Orientation to Obtain S1 and S2 axes parallel and perpendicular to Shear Source Azimuth

Figure 3-6

The desired four-component traces are then given by the following transformations:

$$s_{11} = s_{in,h1}\cos(\phi) + s_{in,h2}\sin(\phi)$$

$$s_{12} = -s_{in,h1}\sin(\phi) + s_{in,h2}\cos(\phi)$$

and

$$s_{21} = s_{cr,h1}\cos(\phi) + s_{cr,h2}\sin(\phi)$$

$$s_{22} = -s_{cr,h1}\sin(\phi) + s_{cr,h2}\cos(\phi)$$

where $s_{cr,h1}$ and $s_{cr,h2}$ represent the horizontal recordings due to the crossline source and $s_{in,h1}$ and $s_{in,h2}$ represent the horizontal recordings due to the inline source.

3.2.5. Picking Arrival Times of Shear Waves

To perform the Alford rotation analysis, it is necessary to identify the time window containing the shear wave first break. In most cases, the Alford rotation will be performed using data from this window, and the information derived regarding the fast direction will be used to rotate the entire trace. For near-surface downhole data, it is not always straightforward to identify the shear wave first break, since there may be noise in the traces, and since there may be interfering arrivals. In particular, even for shear sources, there are always P arrivals due to S to P conversions. In all cases the P arrival will precede the S arrival. For geophones deployed at very shallow depths, the arrivals can be nearly coincident, since there has not been enough time for a significant time lag to develop between the two arrivals.

The selection of the correct shear wave arrival can be facilitated by taking advantage of the nature of the source characteristics. In the downhole survey, data were recorded for dual shear sources that were horizontally opposed to one another. In other words, for the crossline source, a sledge hammer impact was directed on one side of the traction plate, and then an impact was directed on the opposite side of the plate. This data collection scheme was repeated for the inline source. Each shear source generates waves with distinct polarities whereas the first break S to P conversion will have the same polarity, regardless of the directionality of the S source. Horizontally opposed S sources on the other hand yield first break shear arrivals that are 180 degrees out of phase. By plotting side by side pairs of traces that were generated by horizontally opposed sources the shear arrival can be readily distinguished from the P arrival and the shear wave window containing the first break can be robustly chosen. An example of these opposite polarity pairs is shown in Figure 3-7. This procedure was applied to all of the traces.

3.2.6. Analysis of Azimuthal Anisotropy

3.2.6.1. Alford Rotation

The principal time series were computed using the formulae:

$$qs1(t) = \cos^2(\theta)\, s_{11}(t) + \sin(\theta)\cos(\theta)\,[s_{21}(t) + s_{12}(t)] + \sin^2(\theta) s_{22}(t)$$

$$qs2(t) = \sin^2(\theta)\, s_{11}(t) - \sin(\theta)\cos(\theta)\,[s_{21}(t) + s_{12}(t)] + \cos^2(\theta) s_{22}(t)$$

The appropriate angle q is computed by enforcing a condition that minimizes off-diagonal energy. The conditions are:

$$0 = \sin^2(\theta)\, s_{21}(t) + \sin(\theta)\cos(\theta)\,[s_{11}(t) - s_{22}(t)] - \cos^2(\theta)\, s_{12}(t),$$

$$0 = \sin^2(\theta)\, s_{12}(t) + \sin(\theta)\cos(\theta)\,[s_{11}(t) - s_{22}(t)] - \cos^2(\theta)\, s_{12}(t).$$

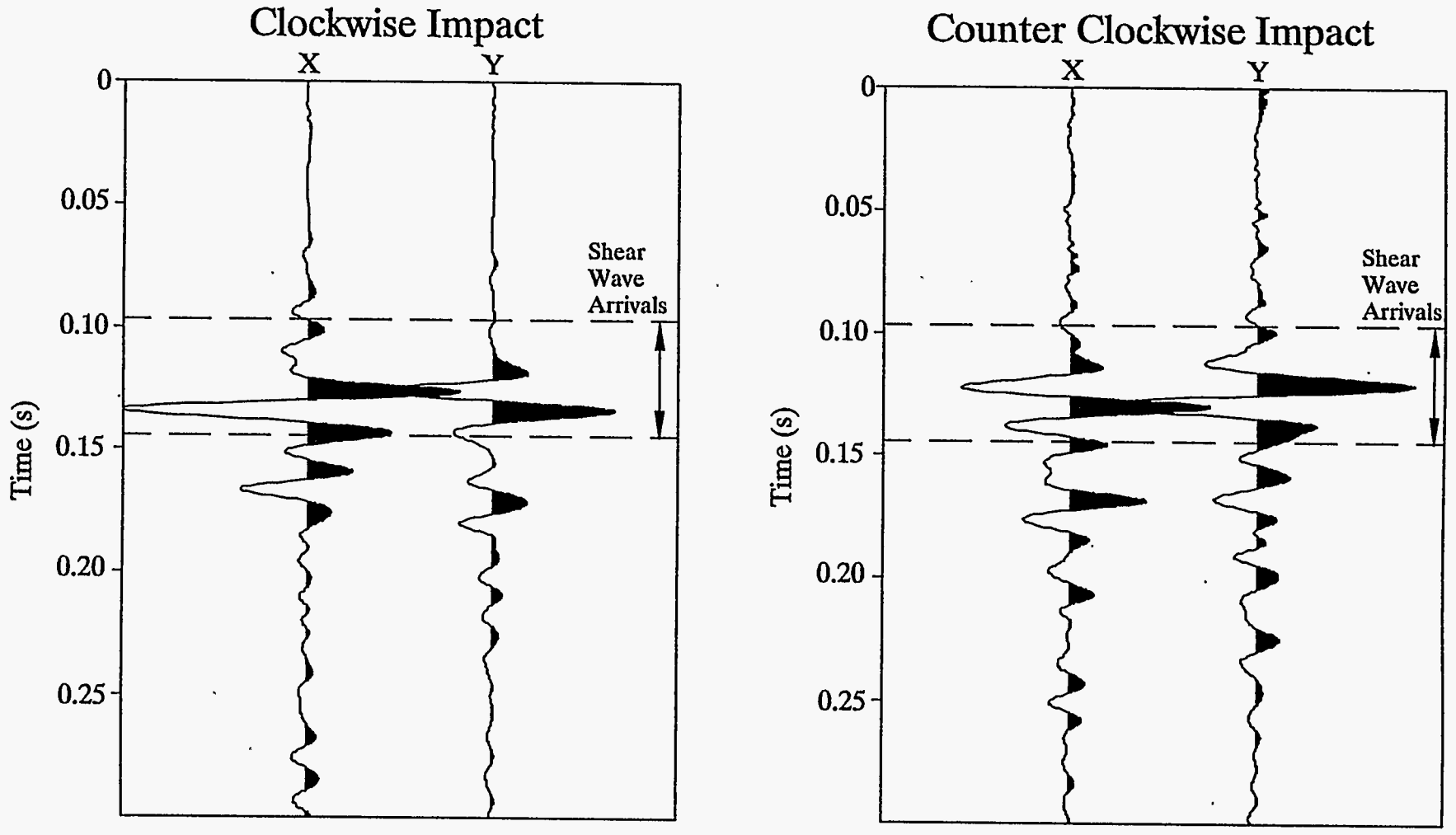

Figure 3-7. Reverse polarities of shear wave arrivals with impact reversal.

It is clear that from the above minimization equations there is an ambiguity in the angle θ; since, for example, a solution θ in the first minimization condition is also satisfied by θ + p/2 in the second minimization condition. In practice, we resolved this ambiguity using the procedure described in the following section.

3.2.6.2. Asynchronous Rotation: The Method of Igel and Crampin

The Alford rotation method is synchronous in that the source and receiver components are corotated. The rotation angle that yields minimal energy in the off-diagonal components of the transformed data is identified with the fast direction. In contrast, an asynchronous rotation method would allow the source and receiver components to be rotated independently of one another. This is more general than the synchronous approach, and the advantage is that it allows for differing fast directions at the source and receiver locations. We applied this method to several pairs of the four-component traces in the downhole data set.

An example of the results from an Igel and Crampin (1990) analysis of the first break is shown in Figure 3-8. The technique can be visualized by first considering the position vector associated with the displacement, $\mathbf{u}(\theta,t)$ at a geophone due to source polarization θ. For each source orientation and each trace in the data set $\mathbf{u}(\theta,t) = (x(t), y(t))^T$ is transformed into a function of direction ϕ (θ,t), where:

$$\phi\ (\theta,t) = \tan^{-1}\ (y(t)/x(t));$$

and the energy in that particular direction:

$$e(\theta,t) = x(t)^2 + y(t)^2$$

A further rearrangement of the seismogram is made by collecting together all of the energies which lie within a particular range of directions ($\phi_i - \delta\phi < \phi < \phi_i + \delta\phi$), to form an energy histogram as a function of direction. If this procedure is repeated for all source polarization's, then a matrix of energy as a function of source polarization θ and horizontal direction f is established. This energy function is termed the *polar energy spectrum*, $F(\theta,\phi)$. Physically, the procedure is equivalent to rotating the source polarization and geophone axes separately and monitoring the recorded energy along a particular direction in the horizontal plane. In the plot above, and in the other graphs, we have plotted $S(\phi)$ which is defined as

$$S(\phi) = \sum F(\theta,\phi) \quad \text{for } 0 < \theta < 180.$$

This sums over all calculated source orientation θ, which we have plotted against the displacement directions ϕ. This function will display maxima in the polarization directions of *qs1* and *qs2*. In Figure 3-8, the maxima in the graph at approximately 145 degrees corresponds to the qs_1 direction. The presence of two clear peaks in the plot that are separated by approximately 90 degrees is a good indicator that azimuthal anisotropy is present.

3.2.7. Cross Correlation's, Time Lags and Removal of Angle Ambiguity

The four-component recordings from shear sources are generated by sources with the same waveform. In anisotropic media, the shear wave immediately splits into fast and slow components. The waveform shape of each component retains the signature of the source waveform, but the pulse shape travel at the fast and slow propagation velocities.

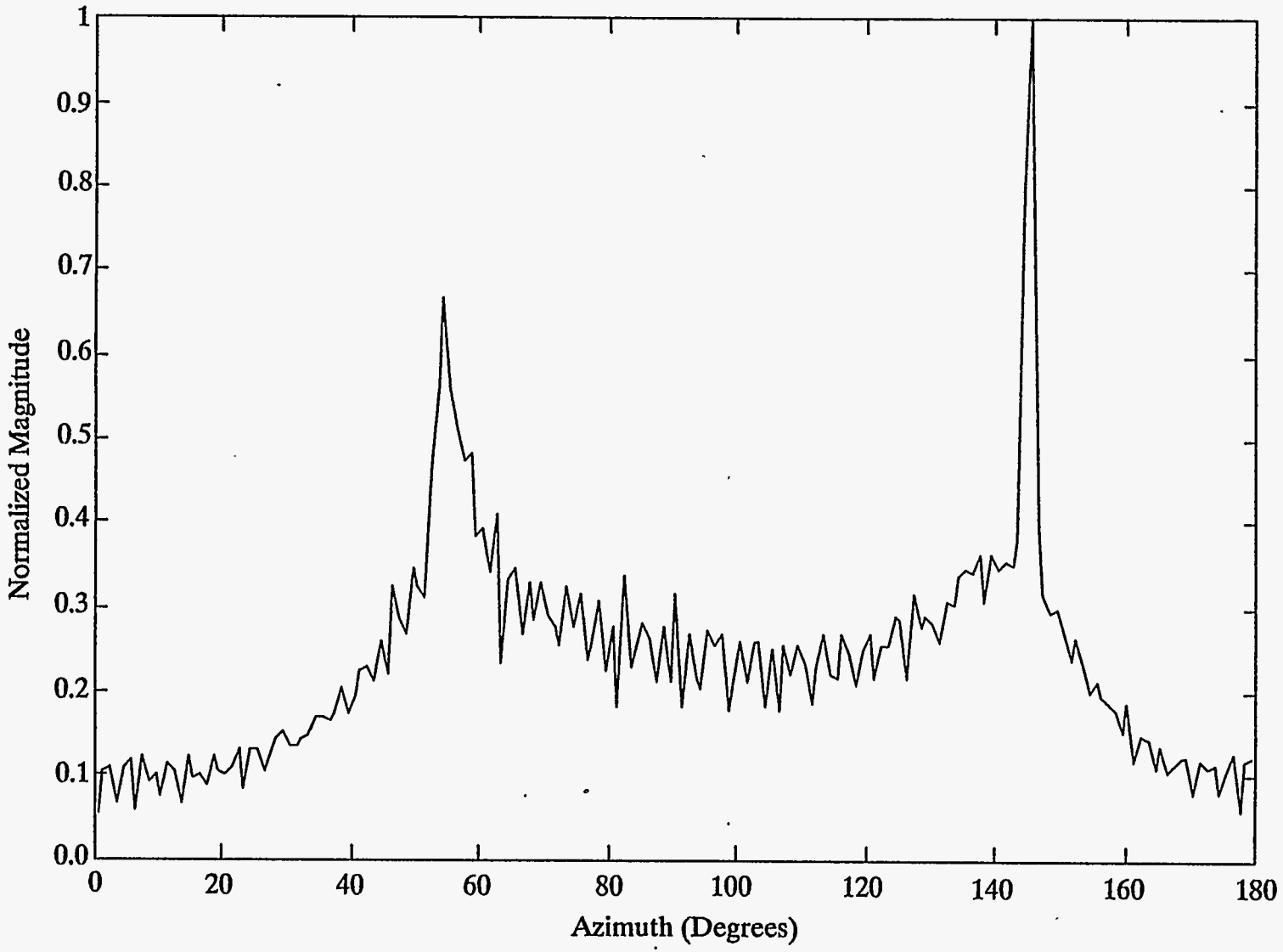

Figure 3-8. Output from Igel Crampin analysis and S_1 Azimuth from Alford rotation Well MSB26A, depth 146 feet

If the anisotropic structure remains coherent along the propagation path, the separations between the waveforms increase with increasing time. The similarity in waveforms can be used to compute objectively the lag time using cross-correlation techniques. To do this, it is first necessary to compute the waveforms along the fast and slow directions. These correspond, of course, to the principal time series *qs1*(*t*) and *qs2*(*t*).

There are a number of ways to perform the cross-correlation, and these depend on the choice of time windows. If most of the energy in the waveforms reside in the first break (i.e. there are minimal scattered arrivals, reverberations, inter-bed conversions, etc.), then it may be appropriate to cross-correlate the entire *qs1*(*t*) trace with the entire *qs2*(*t*) trace. In general, however, it will be necessary to cross-correlate a selected subwindow in the *qs1* trace with a selected subwindow in the *qs2* trace. In practice, we selected a window in the *qs1* trace that contained the major first break. In the *qs2* we selected a window whose mid-point corresponds to the mid-point of the window in the *qs1* trace but which was generally considerably wider. For example, we often used a window with 80 ms width. This choice allows ample accommodation for the slow arrival. By zeroing out the trace outside this window we are able to eliminate spurious high correlation with uninteresting arrivals. The time lag between *qs1* and *qs2* can be computed by determining the peak value of the cross-correlogram and subtracting this from a reference value

One measure of the success of the Alford rotation is by examining the similarity of the computed *qs1* and *qs2* waveforms. Although this can be done visually, the cross-correlogram represents an objective valuation of the similarity. A good wave-form match yields a cross-correlogram with a strong positive peak and the correlation decays rapidly from the peak value in a symmetric fashion.

The cross-correlogram serves an additional purpose as well. In performing the Alford rotation analysis there is an ambiguity in the choice of the fast direction. The two minimization criteria in the previous section yield values of the fast angle θ that differ by plus or minus $\pi/2$. This can only be resolved by prior knowledge, or by comparing the *qs1* and *qs2* waveforms. By definition, the qs1 waveform should lead that of *qs2*. If it does not this indicates that the incorrect angle was chosen. In practice, we computed the principal time series using the angle θ from the first condition and comparing the resulting *qs1* and *qs2* waveforms. The cross-correlogram between *qs1* and *qs2* is computed, and the time lag determined. A positive time lag implies that the *qs1* waveform leads that of *qs2*, and a negative time lag implies that the *qs2* waveform leads *qs1*. Since, *qs1* corresponds to the arrival from the fast direction, we require the lag time to be positive. A negative time lag indicates the incorrect angle was used, and the angle obtained from the second condition implies the correct choice. The computed *qs1* and *qs2* waveforms and their resultant cross-correlation is shown in Figure 3-9.

3.3. Testing Of Multi-Component Processing Algorithms

To verify the correct operation of these algorithms, a synthetic data set was used as input into all the programs. The data set was provided by the University of Edinburgh(Reference) and consisted of a vertical seismic profile(VSP) data set, which modeled 3 component geophone response to orthogonal shear wave sources in a layered anisotropic Earth. In all cases, the programs correctly determined the fast and slow shear wave directions of the model.

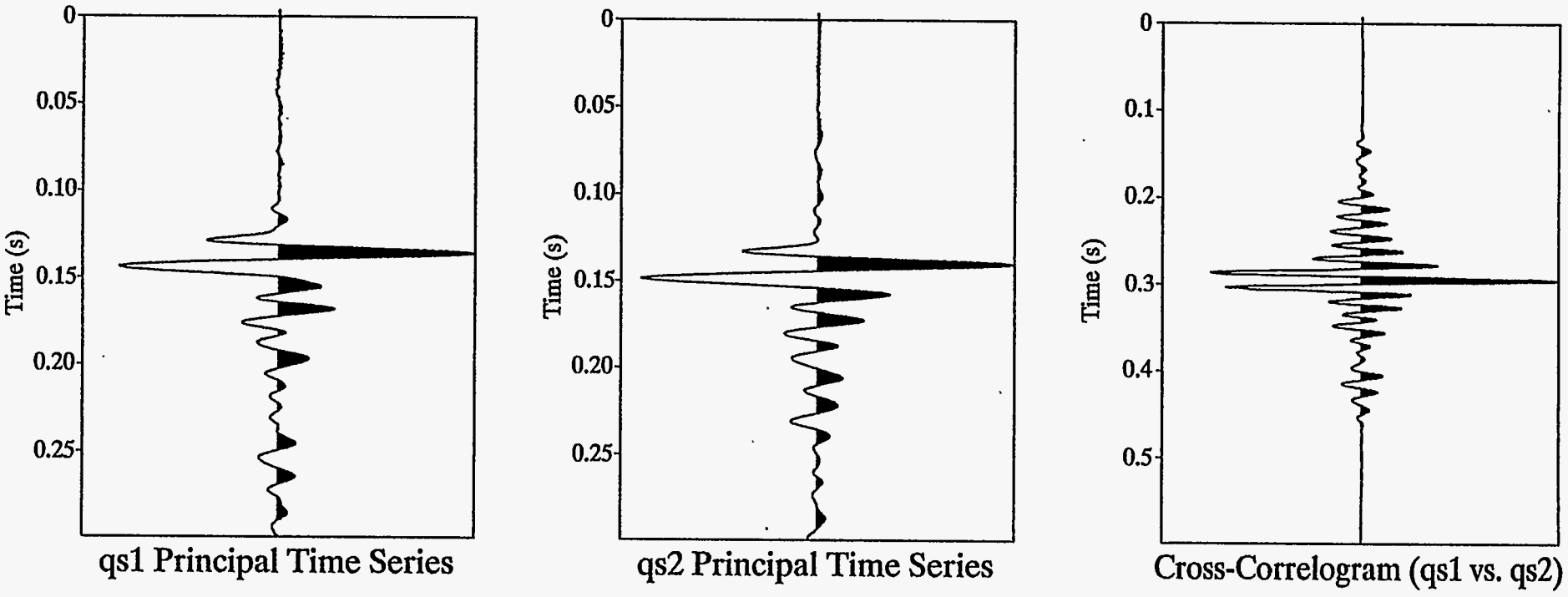

Figure 3-9. qs1 and qs2 Principal Time Series and their Cross-Correlogram
Well MSB21TA - Depth 166 Feet

PROJECTS\ SAVAN5\ SRSACAD\ CORFGRAM DWG

Additional tests to determine the robustness of the algorithms on noisy data. In the case of the synthetic data the traces which correspond to the S_{12} are identical to the S_{21} traces. This, in fact, is the assumption made by most of the algorithms which were used in the analysis of the data. However, this assumption is not true in the data collected in the field.

In order to test the effects of the data asymmetry on the algorithms, S_{12} were multiplied by factor of two. This factor was determined by an analysis of the recorded data. This multiplication had the effect of rotating the fast and slow directions by 5° - 10°. We believe this is likely the accuracy of the angles that can be calculated using these methods.

3.4. Conclusions from Borehole Shear Wave Data Analysis

Our analysis of the downhole shear wave data collected at SRS reaches the following conclusions:

- Seismic azimuthal anisotropy is present in at least two boreholes (MSB21TA and MSB26A), the data quality from the other three boreholes was insufficient to obtain useful results.
- The amount of anisotropy is small (< 4%).
- The qs_1 (fast) axes in the two wells appear to be oriented approximately at approximately 130° to 150°, but that the fast and slow azimuths reverse at approximately the depth of the CBCU.
- The azimuths of the fast direction derived from the Alford Rotation method were within 20° of those obtained from the Igel and Crampin method. However, they were within 10° in Well MSB26A. This may indicate that there was some near surface anisotropic effects at MSB21TA.

3.4.1. Data Quality

The data quality for the first two wells surveyed, MSB21TA and MSB26A, was generally very good, but the data quality for the remaining wells was poor. This poor data quality for the remaining wells was due to several factors including:

- high levels of 60 Hz. noise.
- low frequency and poor quality signal, likely due to poor coupling between the borehole wall and surrounding soils.

Because of the data quality problems associated with the other three wells, only the results from wells MSB21TA and MSB26A will be discussed.

Filtering to remove 60 Hz. noise was ineffective, likely, due to the fact, that the seismic signal also had a significant part of its energy around 60 Hz., and, therefore, removing the noise also removed a large part of the signal.

The problems with poor data quality in several boreholes suggests that other possible methods of deploying geophones in the subsurface such as along with a cone Penetrometer survey. This would reduce the effects of poor borehole wall/soil coupling. In similar surveys conducted in support of hydrocarbon exploration objectives, geophones which were deployed in boreholes and then grouted in. This resulted in very good data quality.

3.4.2. Results from Alford Rotation

The results from the Alford Rotation analysis are provided in Figure 3-10 and 3-11 for wells MSB21TA and MSB26A, respectively. These plots show the resistivity logs, along with interpreted lithologies from drillers logs as well as other sources. Plotted alongside are the computed *qs1* azimuth, the amount of lag time between the *qs1* and *qs2* arrivals, and the percentage of time lag vs. total travel time. Conclusions that can be derived from this data include:

- the presence of shear wave azimuthal anisotropy in the near surface at SRS, with a fast direction(*qs1*) azimuth of approximately 130° -150°, and
- relatively small amounts of anisotropy (< 4%), and
- possible reversing of the fast and slow directions near the top of the CBCU.

The primary azimuth value was derived by averaging the values of the *qs1* azimuth from different source azimuths. In most cases, these values agreed to within 10°. However, in cases of poor data quality where there was a single outlier among the three values, the outlier was thrown out. There were several instances where the *qs1* and *qs2* directions were reversed. This had the effect of changing the *qs1* polarity by 90°. This is likely due to the small time lags present in the near surface at SRS. The small time lags make it difficult to separate the *qs1* and *qs2* arrivals, and therefore make it difficult to determine which orientation arrives first.

The difficulty of determining the absolute *qs1* azimuth is compounded by the difficulty in computing the correct angle to rotate the data into the *qs1* and *qs2* coordinates. This difficulty is seen in Figure 3-6 where three different angles need to be computed to orient the geophones to desired axes, determining an incorrect sign for one of these corrections can lead to incorrect results. This problem is compounded by difficulties in determining the orientation of the direction for positive geophone response. However, these algorithms have now been tested on several different data sets and consistent results have been obtained on all of them. Therefore, we believe the processing flow is correct.

However, the confidence in the results obtained from this analysis is enhanced by the consistency of the results in the azimuth at different depths as well as between different wells. In addition, the *qs1* azimuth is also consistent with azimuths obtained from the Igel and Crampin method discussed below. This is a completely independent method for determining the *qs1* orientation. This is shown in Figure 3-12 where the *qs1* azimuth from the Alford rotation is annotated next to the histogram derived from the Igel and Crampin Method. In well MSB26A, the results for the different depths generally agree to within 10°, which is within the margin of error for these methods.

The reasons for the reversal of the *qs1* and *qs2* azimuths near the top of CBCU are not known at this time. A likely cause for most of the stresses that cause the near surface anisotropy are associated with settling of the sediments and possible slumping of the sediments in towards the Dunbarten Basin. The trends of the Pembrooke Fault and the Cracker Neck Fault System (Figure 3-13) are approximately parallel and orthogonal to the *qs1* and *qs2* azimuths derived from the azimuthal analysis. It is possible that the clays within the CBCU because of the different effective stress due to the water bound to the clays. However, the low values for percent anisotropy suggest that there is very little stress in the upper 200-300 ft. of sediments of the SRS.

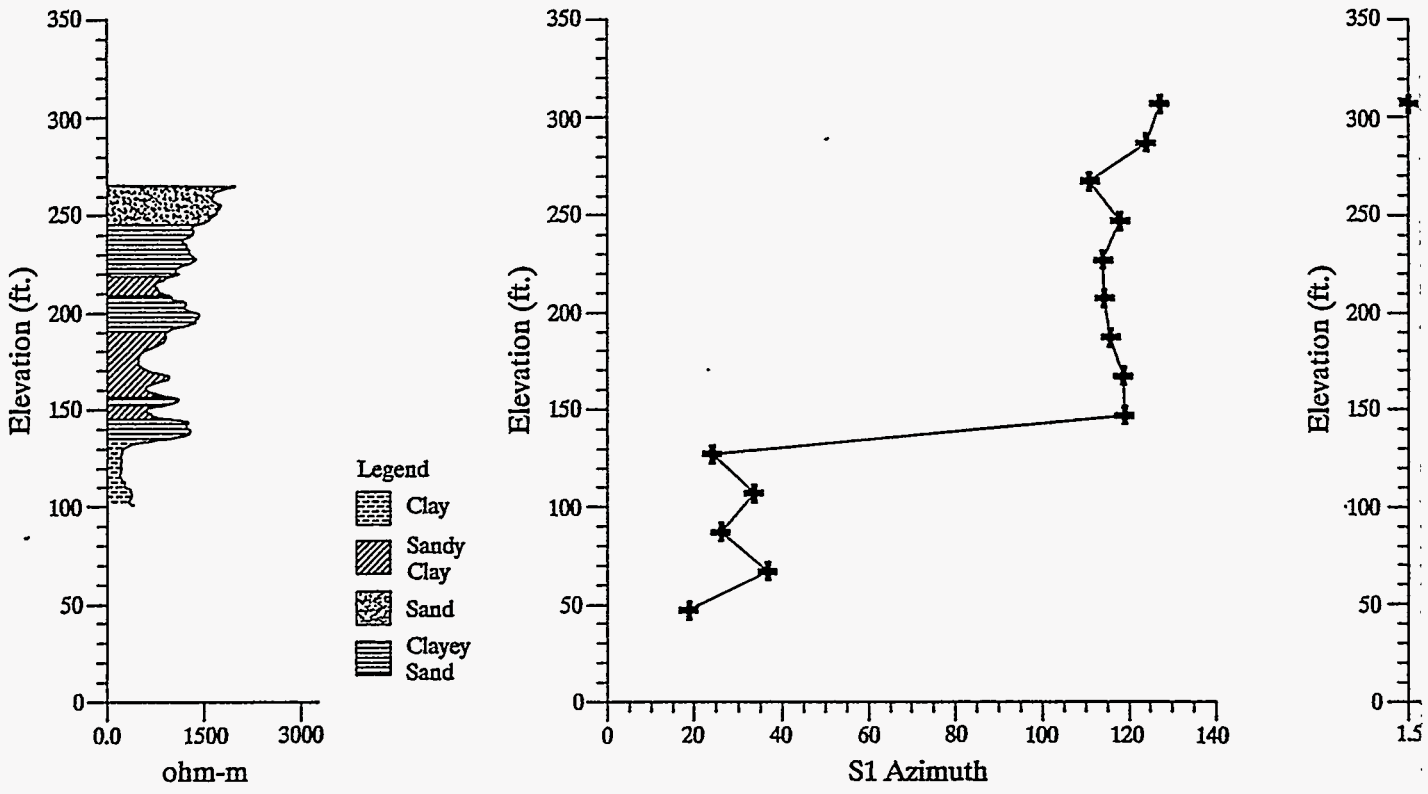

Figure 3-10. Well MS
Lithology and results

S1-S2 Time Lag
Vs. Depth

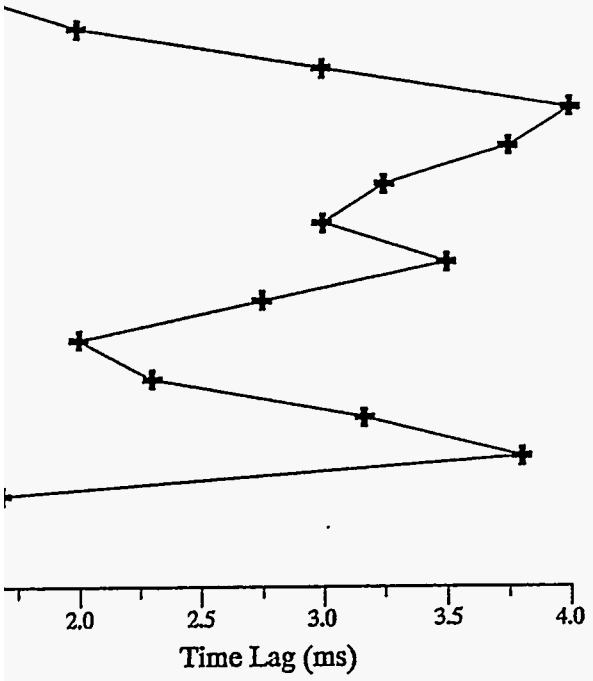

Percent Anisotropy
Vs. Depth

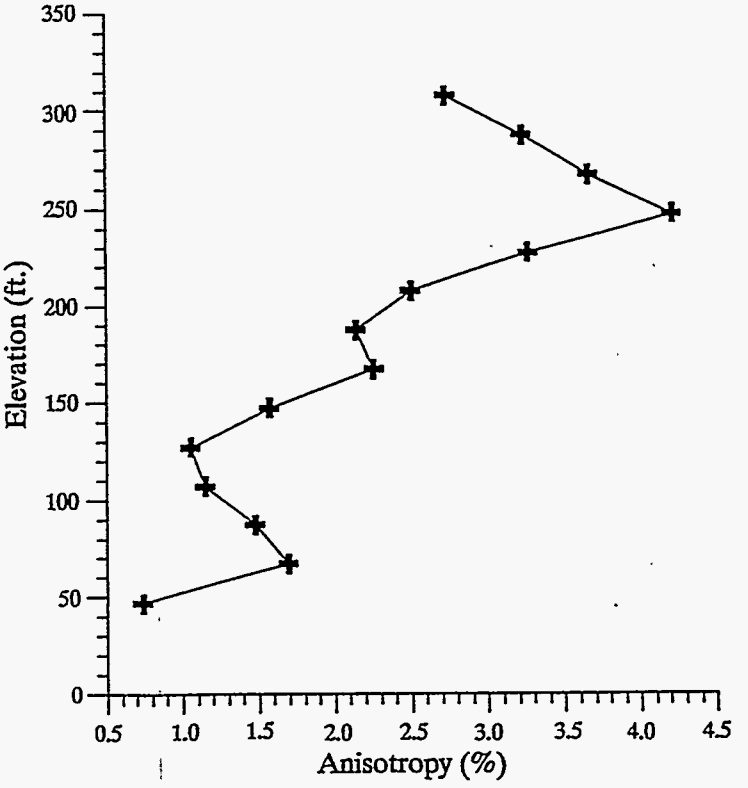

21TA
Alford Rotation Analysis

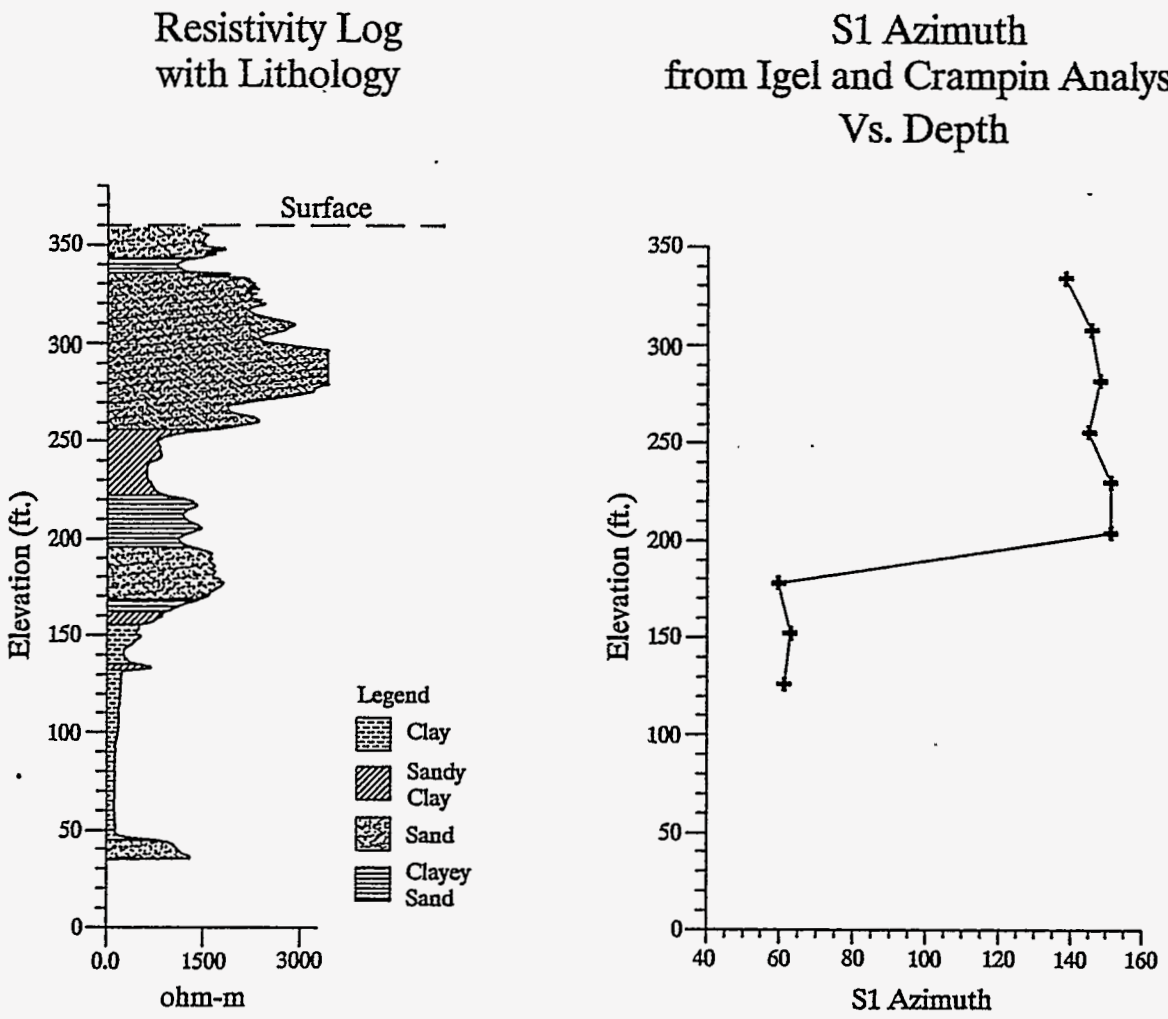

Figure 3-11. Well MS
Lithology and results c

S1-S2 Time Lag
Vs. Depth

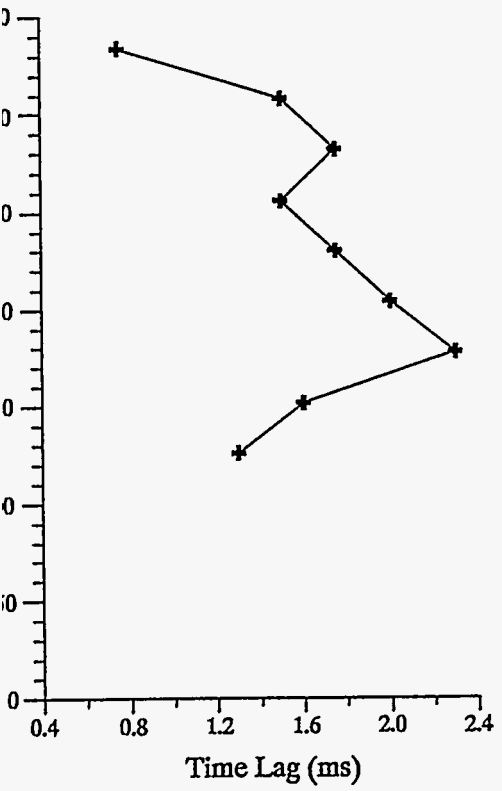

Percent Anisotropy
Vs. Depth

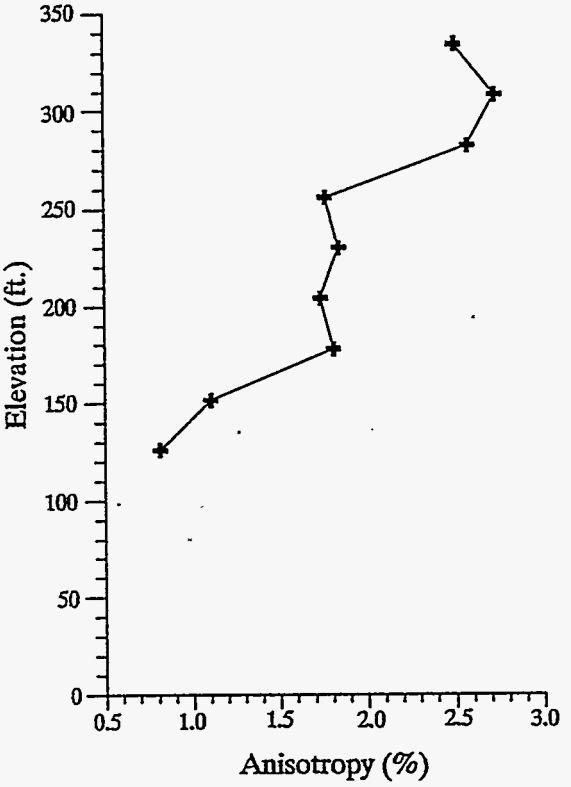

26A
Alford Rotation Analysis

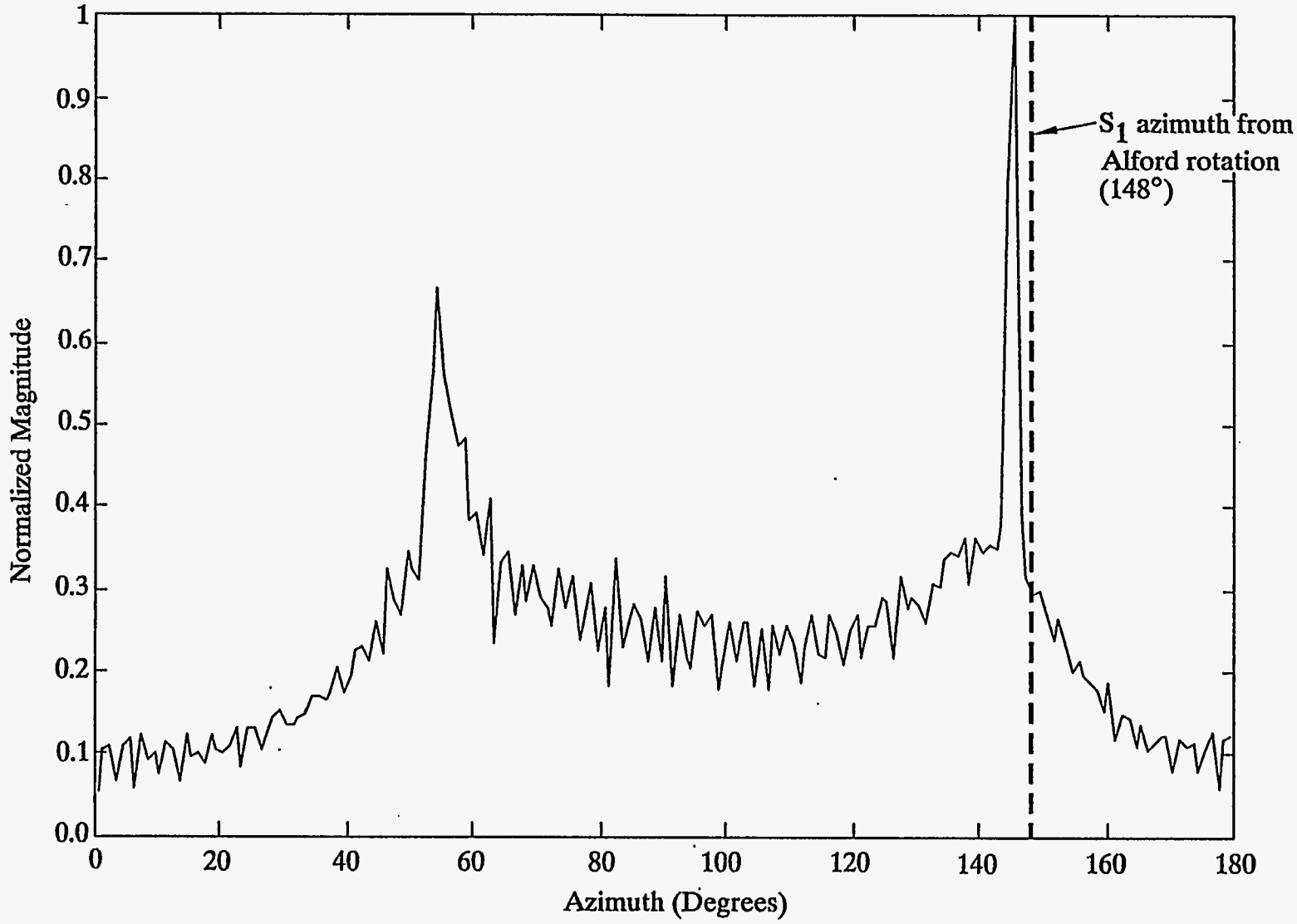

Figure 3-12. Output from Igel Crampin analysis and S_1 Azimuth from Alford rotation Well MSB26A, depth 146 feet

Furthermore, it may not possible to accurately determine the orientation of the *qs1* and *qs2* azimuths in the CBCU is there is a change in their orientation from the overlying layers without layer stripping(Winterstein, 1990). Layer stripping is a technique by which removes the propagation effects of layers overlying the zone of interest. This, however, would require development of additional algorithms.

3.4.3. Results from Igel-Crampin Analysis

The results from the Igel and Crampin analysis are again an indicator of the presence of azimuthal anisotropy. The maxima, which are clearly present in the majority of the data, indicate clearly that shear wave splitting occurs in the near surface. Furthermore, the *qs1* azimuths derived from this method are consistent between the different source azimuths for each depth and for different depths in each borehole.

The output from the Igel and Crampin analysis for the two wells (MSB21TA and MSB26A) at the same depth is shown in Figure 3-14. The difference in the *qs1* azimuth between the two wells is within 15^{o} again an indicator of the presence of azimuthal anisotropy in upper 200 ft. at SRS. The results from the Igel and Crampin analysis in general are more consistent between the boreholes than the Alford analysis. This may be due in part to an anomalous near surface anisotropy near MSB21TA. This is because the independent rotation of the source and receivers in the Igel and Crampin method allow variations in anisotropy near the surface to be removed and primarily the anisotropic conditions near the receivers are being analyzed. Therefore, near surface effects can be removed.

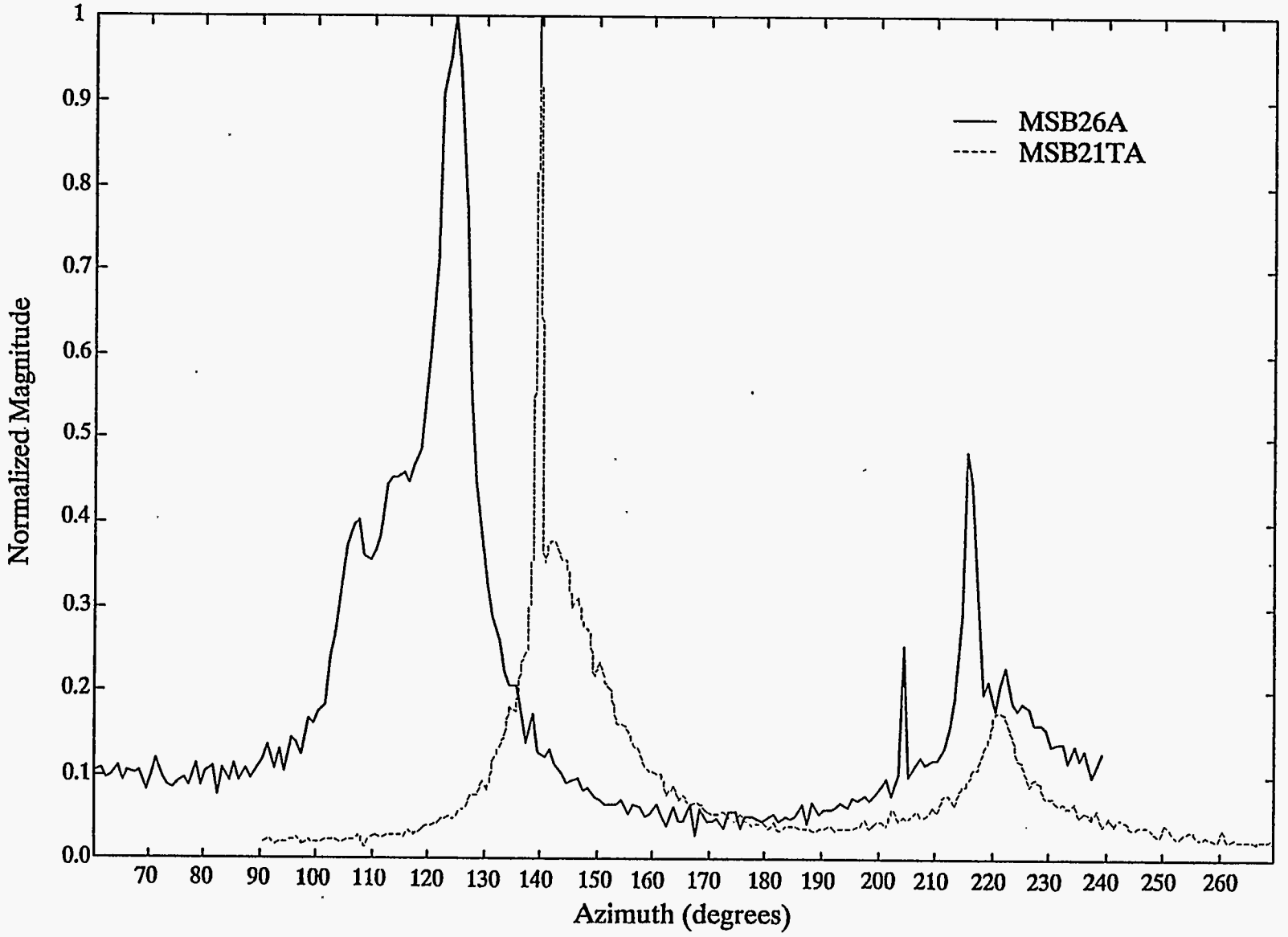

Figure 3-14. Comparison of the results from Igel and Crampin analysis from boreholes MSB21TA and MSB26A at 186'.

4. POTENTIAL FOR COMMERCIALIZATION

Three aspects of the work conducted under DOE Contract DE-AC21-92MC29106 have potential for commercialization. Some of that potential has already been realized on additional government and commercial contracts. Aspects of this work with commercialization potential are :

1. A technical approach for using both electromagnetic and seismic data to define both lithology and stratigraphy of clay confining zones. Clay confining zones have significance in environmental remediation beyond SRS. Establishing continuity of clay confining zones often is a critical objective in site assessment. This work clearly shows the advantage of using shear waves instead of, or in addition to compressional waves for defining stratigraphy.

2. Establishing the clear advantage of minivibrators for performing multi-component seismic reflection surveys. The work at SRS established without doubt the advantages of minivibrators for high resolution seismic reflection surveys. The advantages are:

- Seismic energy of high frequency content can be generated and often recorded.
- Minivibrators can be used for generating both for S-waves and P-waves.
- Minivibrators can be driven over the road to the job site. The large vibrators used in the oil and gas exploration need to be hauled by trailers. This greatly reduces mobilization/demobilization costs.

The minivibrators open large potential for high resolution seismic reflection in shallow investigations, such as for mapping structural geology and geotechnical parameters in coal mining, coal bed methane exploration, environmental site assessment and ground water exploration. A sales brochure recently made for introducing this technology to the coal industry is given in Appendix A.

3. Development of Algorithms for Effective Processing of Shear Wave reflection Data. The vast majority of seismic reflection surveys are performed with P-waves, and as a result computer programs for effective processing of shear wave data is lacking. In this DOE program we have made significant strides in developing computer programs for shear wave analysis. Shear waves will play a greater role in environmental site assessments than in oil and gas exploration and field development.

The capability for analysis of shear waves is actively being marketed for mapping fractures for environmental site assessments in bedrock controlled hydrogeology and for mapping clay layers in unconsolidated sediments.

In summary, the technology developed under this DOE program, allows us to offer services that were hereto not available. Several contracts have already been won and completed.

5. CONCLUSIONS

Reprocessing of the TDEM data by constraining the inversions by the position and structure of stratigraphic horizons obtained from shear wave reflection data results in considerably less equivalence. In particular, the reduction in equivalence in the resistivity of the Crouch Branch Confining Unit allows correlating the absolute value of resistivity to clay content. Clay content, in turn, can be correlated to vertical permeability. This will, however, require acquisition of high quality geophysical borehole logs.

A rich library of software for processing of shear wave data has been developed and tested on multi-component check shot surveys in boreholes. To establish validity of processing code, data were analyzed by a number of different techniques. This new software is already of value in other government and commercial contracts.

The commercial potential for the technical approaches developed under the DOE contract are being proven by award of several government and commercial contracts for projects with similar scope of work.

6. REFERENCES

Alford, R.M. 1986, Shear Data in the Presence of Azimuthal Anisotropy: 56th Ann. Internat. Mtg.,

Soc. Expl. Geophysicists., Expanded Abstracts, 476-479

Domoracki, W.J. 1994, A Geophysical Investigation of Geologic Structure and Regional Tectonic Setting at the Savannah River Site, South Carolina, Ph.D. Thesis, Virginia Polytechnic Institute

Igel, H. and Crampin, S. 1990, Extracting Shear Wave Polarization's from Different Source Orientations: Synthetic Modeling: J. Geophys. Res, **95**, 11 283 -11 292.

Thomsen, L.A., 1988, Reflection Seismology over Azimuthally Anisotropic Media: Geophysics, **53** 304-313

Winterstein, D.F., and Meadows, M.A., 1990, Changes in Shear Wave Polarization with Depth in the Cymric and Railroad Gap Oil Fields: 60th Ann. Internat. Mtg., Soc. Expl. Geophys., Expanded Abstracts, 1435-1438.

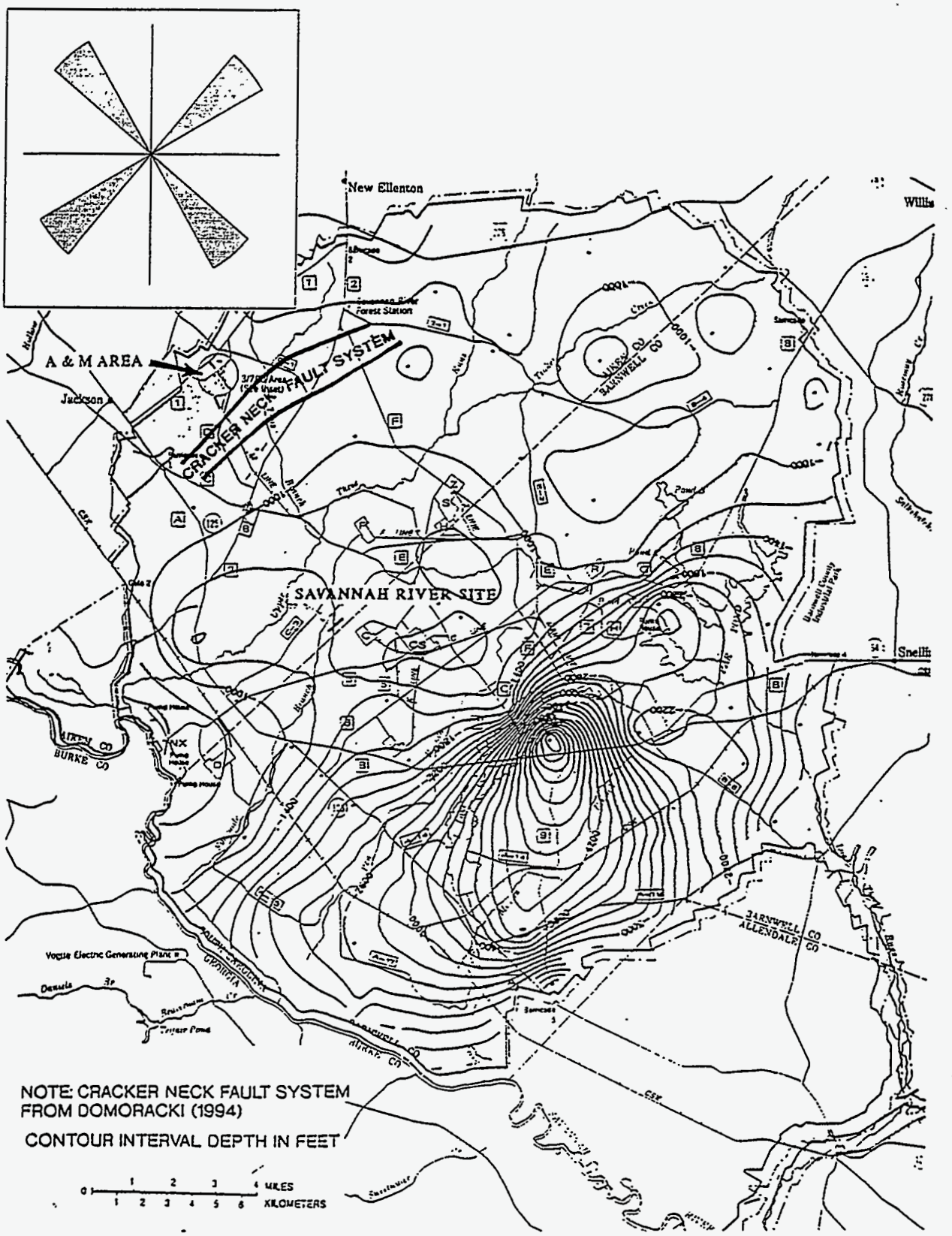

Figure 3-13. Relationship of computed *qs1* and *qs2* azimuths to regional tectonic features at Savannah River Site.